

**THE CHEMICAL TRANSPORT MECHANISM OF EMITTER
MICRO-PARTICLES PARTICLES IN TUNGSTEN
ELECTRODES- A METALLURGICAL STUDY**

Dissertation submitted

In partial fulfillment of the requirements of the degree of

Master of Technology

In

MATERIALS ENGINEERING

By

SABA

(Enrolment No: 16545015)



DEPARTMENT OF METALLURGICAL AND MATERIAL SCIENCE

INDIAN INSTITUTE OF TECHNOLOGY ROORKEE

ROORKEE-247667 (INDIA)

MAY, 2018

CANDIDATE'S DECLARATION

I hereby declare that the work presented in dissertation entitled "The Chemical Transport Mechanism of Emitter Micro-Particles in Tungsten Electrodes-A Metallurgical Study" submitted in partial fulfillment of the requirements for the award of degree of Master of Technology in Materials Engineering, Indian Institute of Technology Roorkee, is an authentic record of my work carried out under the supervision of Prof. Dr. Habit. Uwe. Fuessel, Chair of Joining Technology and Assembly, Institute of Manufacturing, TU Dresden, Germany, Dr. P.K Ghosh, Associate Professor, and Dr. Sorav Das, Assistant Professor, Department of Metallurgical and Materials Engg., IIT Roorkee The matter embodied in this has not been submitted by me for the award of any other degree.

Saba

Enrolment No. 1645015

Date:

CERTIFICATE

This is to certify that the above statement made by the candidate is correct to the best of my knowledge.

Dr. Sorav Das

Assistant Professor

MMED Department

Indian Institute of Technology

Roorkee, India

Dr-Ing. **habil.** Uwe Fuessel

Professor

Prof. Dr.-Ing. habil. Uwe Fuessel

Chair of **joining** Technology and Assembly

Institute of Manufacturing Technology

Technical University of Dresden, German

Technische Universität Dresden

Fakultät Maschinenwesen
Institut für Fertigungstechnik
Professur für Fügetechnik und Montage
01062 Dresden

ACKNOWLEDGEMENTS

I thank all who in one way or another contributed in the completion of this thesis. First, I give thanks to God for protection and ability to do work.

I would like to express my deepest sense of Gratitude to my supervisors **Prof. Dr.-Ing. Habil. Uwe. Fuessel**, Chair of Joining Technology and Assembly, Institute for manufacturing Technology, Technical University of Dresden and **Prof. P.K Ghosh and Dr. Sorav Das**, Department of Metallurgical and Materials Engineering, Roorkee (India), for their continuous advice and encouragement throughout the course of this thesis. I thank them for the systematic guidance and great effort they put into training me in the scientific field.

In particular I would like to thank **Mr. Henning Schuster**, Dipl. Ing., for the guidance, encouragement and advice he has provided throughout my time as his student. I am indebted to him for his constant support.

I am also so thankful to **Mr. Gurjit Singh**, PhD Research Scholar, whose challenges and productive critics have provided new ideas to the work. I really appreciate his technical as well as moral support during my research.

I would like to also acknowledge all the staff, **Dr. Michael Pejko** and **Frau Karin Jaeger** for all their technical support. You definitely provided me with the tools that I needed to choose the right direction and successfully complete my dissertation.

I want to thank DAAD (**Deutscher Akademischer Austauschdienst**) for its financial support during my stay and excellent cooperation to conduct my research at Technical university of Dresden.

I would also like to thank my **parents** for their wise counsel and sympathetic ear. You are always there for me. Finally, there are my **friends**. We were not only able to support each other by deliberating over our problems and findings, but also happily by talking about things other than just our research work.

Thank you very much, everyone!

SABA

ABSTRACT

A metallurgical study has been conducted on the erosion mechanism of pure tungsten electrodes and 1.5% La_2O_3 doped tungsten electrodes, used in Tungsten Inert Gas (TIG) welding. The behavior of micro-emitter particles in Lanthana doped electrodes has been studied from the points of view of in-process electrode consumption, topographical changes on electrode, the formed phases evaluation and electrode temperature profile estimation by using various materials characterization techniques. The results show various characteristics zones on the surface of tungsten electrode tip, which signifies the difference in the migration and evaporation of lanthana emitter particles. Due to difference in working temperature inside the electrode, variation in grain growth occurred in both type of electrodes. Also, it has been observed that the Lanthana doped electrode durability decreases with time due to consumption of emitter particles and temperature dependant grain coarsening of tungsten matrix.



TABLE OF CONTENT

TABLE OF CONTENT.....	iv
1. INTRODUCTION.....	1
2. THEORETICAL BACKGROUND AND LITERATURE OVERVIEW	3
2.1 Tungsten inert gas arc welding (TIG).....	3
2.1.1 Basic mechanism of TIG welding:.....	3
2.1.2 Types of welding current used in TIG welding	5
2.1.3 Advantages of TIG welding.....	6
2.1.4 Disadvantages of TIG Welding.....	6
2.1.5 Applications of TIG Welding	6
2.2 Zones in welding arc and their roles	7
2.2.1 Cathode spot:.....	7
2.2.2 Cathode drop zone: :.....	8
2.2.3 Plasma:.....	8
2.2.5 Anode spot:	8
2.3 Electrodes used in TIG welding.....	8
2.4 Emission of electrons and its mechanism.....	10
2.5 Effects Due To High Temperature on Erosion of Tungsten Electron in TIG Welding	12
2.6 Erosion of electrodes.....	13
3.1 Requirement of the experimental work	17
3.2 Planning of the Experimental work	19
4. DESIGN OF EXPERIMENTAL WORK.....	21
4.1 Equipment for Arcing-	21
4.2 Tip Surface topography examination by optical microscopy and scanning electron microscopy	23
4.3 Elemental analysis of tip surface by EDX.....	24
5. RESULTS AND DISCUSSION	26
5.1 Stability/durability of the electrode tip geometry	26
5.2 Scanning electron microscopy and EDX analysis of electrode tips	28
5.2.1 Scanning electron Microscopy of La ₂ O ₃ doped Tungsten electrodes	28
5.2.2 Scanning electron microscopy of Pure Tungsten electrodes	34
5.3 Cross sectional study of pure W electrode tips.....	38
5.3.1 Optical microscopy of electrode tip cross section.....	38
5.3.2 SEM of electrode tip cross section.....	41
5.4 Cross sectional study of Lanthanum oxide doped electrode tips.....	41

5.4.1 Optical microscopy of electrode tip cross section.....	41
5.4.2 SEM of Lanthanized electrode tip cross section.....	44
5.5 X-Ray Diffraction for Phase Analysis	46
6. CONCLUSION	48
7. REFERENCES.....	60



LIST OF FIGURES

Figure 2.1: Schematic Diagram of TIG Welding System[4].....	4
Figure 2.2: Principle of TIG Welding [5].....	4
Figure 2.3: Various Zones in arc gap of a welding arc[10].....	7
Figure 2.4: Potential drop as function of distance from cathode to anode[10].....	7
Figure 2.5: Effect of different dopants on Arc Pressure.....	13
Figure 2.6: Metallurgical microstructure of an electrode cross section after heavy loading.....	13
Figure 2.7: Electrode tip Appearance.....	14
Figure 2.8: Erosion rate as a function of arc current and ambient pressure.....	14
Figure 2.9: Erosion rate as a function of electrode diameter.....	15
Figure 2.10 Change in electrode tip shape due to long time operation ($\text{La}_2\text{O}_3 + \text{CeO}_2 + \text{Y}_2\text{O}_3 = 2\%$).....	15
Figure 2.11: Typical macrostructure of tungsten electron activated with combined additives of rare earth metal oxides after 10 hr arcing at 180A A in pure Ar.....	15
Figure 2.12: Erosion rate on arc current Intensity in conical cathodes. Arcing time = 5 min.....	16
Figure 3.1: Steps followed for evaluating behavior of rare earth oxides.....	20
Figure 4.1: View of welding machine used for arcing.....	21
Figure 4.2: La Doped Electrode tips after welding for different arcing time.....	23
Figure 4.3: Schematic plan for SEM and EDX experiment.....	24
Figure 5.1: Electrode tip appearance after 1, 2 and 3 performing weld cycles.....	26
Figure 5.2: Electrode tip appearance after 6, 9 and 12 weld cycles.....	27
Figure 5.3: Electrode tip appearance after 15, 18 and 21 weld cycles.....	27
Figure 5.4: Characteristics zones observed in La electrode tip surface in SEM.....	28
Figure 5.5(a): Microstructural View of Zone A and B after N=9 and 18.....	29
Figure 5.5(b): Figure 5.5(b): Microstructural View of Zone A and B after N=21	29

Figure 5.6(a) : EDX mapping of zone A after N=3.....	30
Figure 5.6(b): EDX analysis of different zones observed in La₂O₃ doped electrode tips.....	31
Figure 5.7: Microstructure of crystallization zone C.....	31
Figure 5.8: Formation of La deposit ring on the upper cylindrical part of electrode.....	32
Figure 5.9(a): EDX analysis of ring formed on the cylindrical part.....	32
Figure 5.9(b): EDX mapping of La deposit ring on the upper cylindrical part of electrode.....	33
Figure 5.10: Magnified view of different regions in pure tungsten electrode after 10 minutes of arcing.....	34
Figure 5.11: Pure tungsten electrode tips under SEM after arcing for different weld cycles.....	35
Figure 5.12: Magnified view of emission Region (a).....	36
Figure 5.13: Magnified side view of Region (c) in electrode tip after different weld cycles(N...)	36
Figure 5.14: Magnified view of Region (c) after different weld cycles(N).....	37
Figure 5.15: Region on polished electrode tip cross section for optical microscopy.....	38
Figure 5.16: Metallurgical microstructures of an electrode cross section of unused electrode and after 2 weld cycles.....	38
Figure 5.17: Metallurgical microstructures of an electrode cross section after 6 and 12 weld cycles.....	39
Figure 5.18: Metallurgical microstructures of an electrode cross section after 18 weld cycles.....	39
Figure 5.19: SEM micrographs of pure tungsten electrode tip after different weld cycles (N)....	40
Figure 5.20: Magnified view of electrode tip cross section at higher weld cycles.....	41
Figure 5.21: Optical microstructure of La doped electrode tips after 30 minutes of arcing (N=6).....	43
Figure 5.22: Optical microstructure of La doped electrode tips after 60 minutes of arcing (N=12).....	43
Figure 5.23: Microstructure of Lanthanised tip cross section after 12 and 18 weld cycles.....	44

Figure 5.24: EDX mapping of electrode tip and core of electrode cross section after 12 and 18 weld cycles.....45

Figure 5.25: Elemental mapping at the center of electrode cross section after N=12.....45

Figure 5.26: Standard XRD data of pure tungsten from IBSD database.....46

Figure 5.27: XRD analysis for Lanthanized electrodes after different weld cycles.....47



LIST OF TABLES

Table 1: Color codes and alloy element contents of tungsten electrode alloys [13].....	10
Table 2: Change in Tip Temperature and Work function as a function of lanthana content	11
Table 3: Electrodes with different arcing time and corresponding weld cycles.....	19
Table 4: Welding parameters for arcing.....	22



1. INTRODUCTION

The tungsten electrode, used as cathode terminal in TIG welding for generating the welding arc, undergoes various wear processes during work life. Such processes are for example the thermal erosion as a result of the very high surface temperatures due to the thermionic work conditions. Technically, this non-desirable phenomenon is controlled by the attempt to lower the service temperature of the electrode. Such influence of service temperature can be achieved by adding some rare earth metal oxides as emitter micro particles in tungsten matrix [1]. Rare earth elements and its oxides show a significantly lower work function than pure tungsten, which allows the significant lowering of the service temperature for the thermionic emission of the tungsten electrode. Commonly used rare earth oxides for such implementation are La_2O_3 , ThO_2 , Y_2O_3 , CeO_2 and ZrO_2 .

The oxide particles doped tungsten electrodes show superior characteristics, compared to pure tungsten electrodes, in their operation. These advantageous conditions in service is the result of the comparatively lower work function of the rare earth element oxides. Rare Earth Oxides also show lower melting temperatures than pure tungsten. Such significant differences in thermal properties results in migration process (chemical transport) of these particles. The migration processes are temperature, concentration and time dependent, vectored from lower temperature zone to higher temperature zone along the grain boundaries. Also capillarity driven forces take place for transport of liquid phase oxides from the near tip electrode core up to the tip region. Ideally this migration process is beneficial, as it can provide the same emission rate as that of pure tungsten, with significantly lower working temperature of the cathode. As these oxides reach the zone of highest temperature at the surface of the electrode tip, evaporate.

With the loss of emissive oxide particles due to evaporation from the electrode tip surface, an increment in the electrode working temperature takes place. The electrode tip behaves more in a state of a pure tungsten type at that time. The increment in tip temperature causes additional effects like the change in shape of grain boundaries from longitudinal to granular, due to which the number of grain boundaries decreases. Resulting the change of grain size and structure, the diffusion rate of oxide particles along the grain boundaries decreases and takes more time to reach the electrode surface[2].

It is still not well understood how the rare earth particles influences erosion mechanism and working temperature of the electrode. Thus, for developing certain methods to improve the life of electrodes it is very important to study the mechanism of erosion in a more detailed manner. With a span of time, due to very high working temperature and after the loss of oxide particles, tungsten also starts evaporating from the electrode surface and causing the erosion of the electrode surface. This process finally leads to the change in tip geometry, poor arc starting characteristic, and shape of the arc. The service life of a tungsten electrode is limited by the conditions of the arc establishment. Changes of tip-geometry or service temperature for electron emission severely influences the characteristics of the established arc and causes a reduction in process stability.

The present work aims to study about the mechanism of chemical transport of emitter micro particles in La oxide doped tungsten electrode and in pure tungsten electrode during real service conditions. In the experimental work, the micro structure of the used electrode's tip surface after different weld cycles were studied by optical microscope, scanning electron microscope and EDX in order to gauge the extent of the diffusion of concerned particles reaction. And the resultant phases formed will be studied by reflective XRD.



2. THEORETICAL BACKGROUND AND LITERATURE OVERVIEW

2.1 Tungsten inert gas arc welding (TIG)

TIG welding was developed during 1940s at the start of the Second World War. The TIG development intended to improve the welding of material with low or no weldability for traditional welding processes, for example aluminum and magnesium alloys. The use of TIG today has spread for welding of a variety of metals like high tensile steels, light and heavy metals of all kind.

Arc welding is a technique to melt and join different materials using the energy of an electric discharge for heat introduction that is widely used in the industry. The TIG process is also sometimes referred to as Gas Tungsten Arc Welding (GTAW), or heliarc process. Under the correct welding conditions, no melting takes place in the tungsten electrode and is considered to be non-consumable. Filler metal is added by dipping the end of a filler rod into the edge of the molten weld pool or a continuous wire feeding is used [3].

An inert gas, typically argon, flows out of the welding torch, surrounding the hot tungsten and weld pool provide shielding to them from atmospheric oxygen. Although most other welding processes are faster and less expensive, the clean, neat, slag-free welds TIG welds are used. For that reason, it is widely used in industrial applications such as nuclear industry, aircraft industry, food industry, maintenance and repair work.

2.1.1 Basic mechanism of TIG welding:

Tungsten Inert Gas welding is an arc welding process that uses an electric arc, generate between non-consumable tungsten electrode and an anode to produce the weld. The weld area is protected from atmosphere by an inert shielding gas (argon or helium), and a filler metal is commonly added. The welding current is supplied from the power source (Inverter, rectifier, transformer), through welding torch and is delivered to a tungsten electrode. The tungsten electrode is clamped inside the torch to provide a low electric and thermic resistance during operation.

An electric arc is then established between the tungsten electrode tip and the anode i.e. work piece. The welding arc is an electrical discharge caused by flow of current between the



electrodes. This flow of current requires column of charge particles in the form of ions and electrons. A column of highly ionized gas and metal vapours introduces the thermal and electric energy into the work piece.

Due to the high energy density, the electric arc can produce temperatures of up to 15,000°C inside the discharge column. The so created weld pool can join the base metal just directly with the help of added filler material. Schematic picture of TIG welding and mechanism of TIG welding are shown in fig. 1 & fig. 2 respectively.

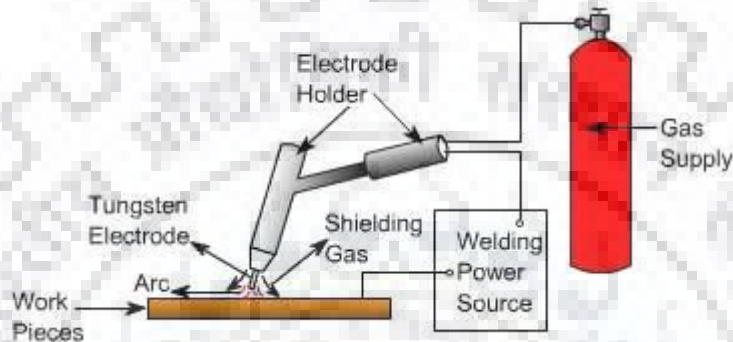


Fig. 2.1 Schematic Diagram of TIG Welding System[4]

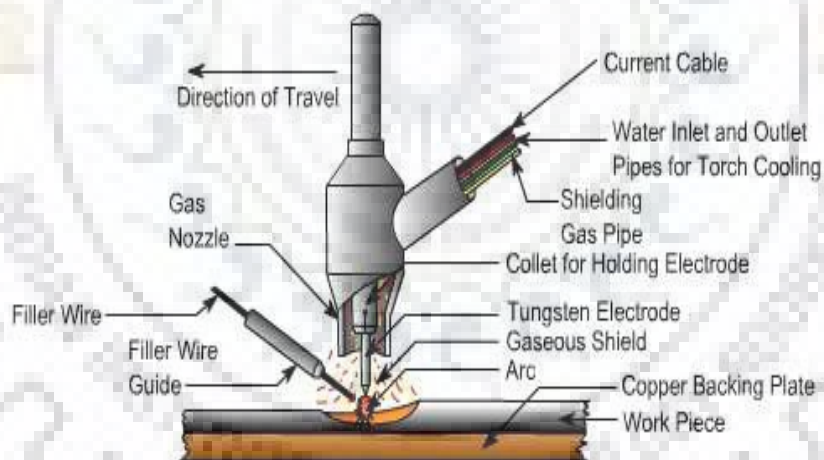


Fig.2.2 Principle of TIG Welding [5]

Tungsten electrodes for TIG welding are commonly available from 0.5 mm to 8.0 mm diameter and up to 200 mm length. The electric current carrying capacity of an electrode depends on its polarity during welding. For most welding purposes, the tungsten electrode poling is negative. For welding Aluminium and Magnesium alloys, the use of alternating current AC is used. In rare and special cases the tungsten electrode is connected with positive potential. The thermal load for the so contacted electrode is extremely high, which is limiting the maximum deliverable current.

The capacity to limit the current to the set value is equally crucial when the electrode is short circuited to the work piece, otherwise excessively high current will flow, damaging the electrode. Open circuit voltage of power source ranges from 60 to 80 V and is limited for security reasons to 113V. In process, the arc voltage is reaching typical values of less than 30 Volts.

2.1.2 Types of welding current used in TIG welding

Different types of welding current can be used in TIG welding as shown below [6]:

- a. **DCEN (*Direct Current Electrode Negative*)**: In this type of TIG welding direct current is used. Tungsten electrode is connected to the negative terminal of power source. This type of connection is the most common and widely used DC welding process. With the tungsten being in DCEN polarity, it will only receive 30% of the welding energy heat [5]. The resulting weld shows good penetration and a narrow profile.
- b. **DCEP (*Direct Current Electrode Positive*)**: In this type of TIG welding polarity used, the tungsten electrode is connected to the positive terminal of power source. This type of connection is used very rarely because of the excessive thermal load of the electrode. DCEP is mainly used on Aluminium and Magnesium alloys at low current.
- c. **AC (*Alternating Current*)**: It is the preferred welding current for metals which have higher affinity towards oxygen, e.g. aluminium and magnesium. AC polarity offers advantages of both DCEN and DCEP; however, to some extent. With AC power source, in half of the cycle electrode becomes negative and in next half of the cycle, electrode becomes positive. Due to change in polarity, cathodic cleaning of surface and heat introduction takes place separately. On the first half cycle, where the tungsten electrode is positive, electrons will flow from work piece to the electrode. This will result in the spattering of any oxide layer on the base material. This side of the wave form is called the cleaning half-wave. As the polarity changes, the electrons will flow from electrode to the work piece. This half cycle is called the penetration half of the AC wave forms.

This cycle repeats 50 or 60 times depending on the frequency (50Hz or 60Hz). Some power sources also provide provisions to alter this frequency. AC polarity offers following benefits:

1. Arc cleaning action.



2. Compatible with most of the electrode types (but not all).
3. Better fusion and weld metal penetration.
4. Suitable for a wide range of plate thickness.

2.1.3 Advantages of TIG welding

TIG welding process has specific advantages over other arc welding process as follows [7] -

1. There is no use of flux, hence no chances of flux entrapment when welding is done for refrigerators and air conditioner components.
2. Visibility of arc and job is very clear, hence provides a better control on welding.
3. Smooth and sound welds can be produced by this process in all positions, with very less spatter.
4. TIG welding is very much useful for thin materials with high quality welds.

2.1.4 Disadvantages of TIG Welding

1. Sometimes tungsten droplets may transfer to molten weld pool, that causes defects in the weld like inclusions which is hard and brittle in nature.
2. Filler rod may come out of the inert gas shield while doing welding that can also cause contamination in the weld pool.
3. High equipment costs.

2.1.5 Applications of TIG Welding

TIG welding can also be used for thicker material plate by using multi passes which results in high heat inputs, and leads to increment in the distortion and reduction in mechanical properties of the work piece. In TIG welding, because of high degree of control in heat input and filler additions separately, high quality welds can be achieved [8]. Also, it can be performed in all positions making it suitable for tube and pipe joint. The TIG welding is a highly controllable and clean process with little or no need for finishing and can be used for both manual and automatic operations. The TIG welding process is extensively used in the so-called high-tech industry applications such as

- Nuclear industry
- Aircraft industry
- Food processing/ Pharmaceutical industry
- Maintenance and repair work



- Precision manufacturing industry
- Automobile industry

2.2 Zones in welding arc and their roles

Once the arc is established, there is a drop in arc voltage across the arc gap. This drop in arc voltage varies with distance from the electrode tip to the weld pool.

Depending on the way by which the potential drop varies between electrode and base metal, arc gap can be divided into five different zones

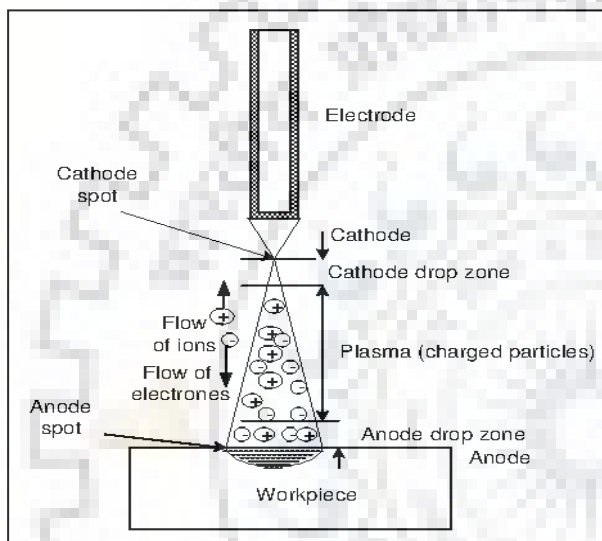


Fig 2.3: Various Zones in arc gap of a welding arc[10]

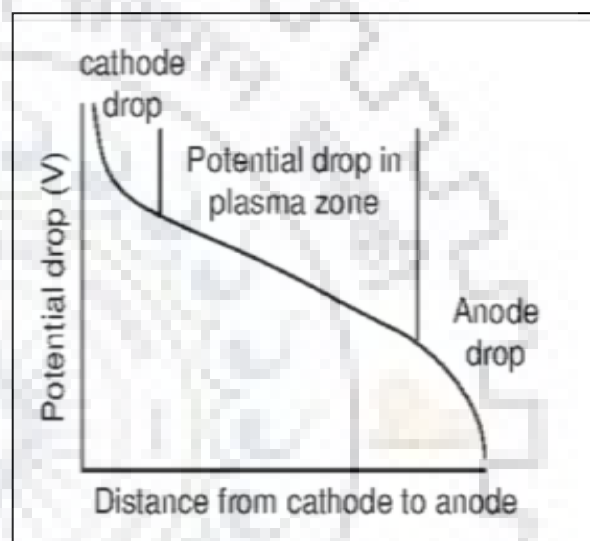


Fig2.4: Potential drop as function of distance from cathode to anode[10]

2.2.1 Cathode spot:

This is a region of cathode from where the electrons are emitted. Two types of cathode spots are generally found namely mobile and pointed. Mobile cathode spot is generally found during the welding of aluminum and magnesium.

This type of cathode spot loosens the oxide layer on reactive metal like aluminum, Mg and stainless steel. Therefore, mobile cathode spot helps in cleaning action when reverse polarity is used i.e. work piece is cathode. Pointed cathode spot is formed at a point only in most of tungsten inert gas welding at lower current densities. A Pointed tungsten electrode forms the pointed cathode-spot [9].



2.2.2 Cathode drop zone: :

This is the region that is very close to the cathode and a very sharp drop of voltage takes place in this zone due to electron-cooling effect of cathode.

Voltage drop in this region directly affects the heat generation near the cathode which in turn governs melting rate of the electrode in case of the consumable arc welding process with straight polarity (electrode is cathode).

2.2.3 Plasma:

This is the region between electrode and work where mostly flow of charged particles namely free electrons and positive ions takes place. In this region, uniform linear voltage drop, like an ohm resistor takes place. Heat generated in this region has minor effect on melting of the work piece and electrode.

2.2.4 Anode drop zone:

Like cathode drop region, anode drop region is also very close to the anode and a very sharp drop in voltage takes place in this region due to cooling effect of the anode. The Voltage drop in this region affects the heat generation near the anode & so melting of anode. In case of direct current electrode negative (DCEN), voltage drop in this zone affects melting of the work piece.

2.2.5 Anode spot:

This is the region of an anode where electrons get merged and their impact generates heat (by recombination reaction) for melting. However, no fixed anode spot is generally noticed on the anode like cathode spot.

2.3 Electrodes used in TIG welding

The function of an electrode in TIG process is to serve as one of the electrical terminals of the arc that supplies the heat required for welding. Since a temperature of around 4000°C is generated in the arc during welding, the role played by the electrode is crucial. Clearly it must have a high melting point and it must be non-consumable. Tungsten quickly established itself as the most suitable material for electrodes in arc welding due to its high melting point and strong electron emission ability. As the knowledge of arc characteristics increased, it became clear that the use of pure tungsten presented some limitations on process development, particularly arc initiation, stability and electrode wear.



The emission efficiency of pure tungsten electrode is too low and the electrode might be fractured for the recrystallization and formation of equiaxed grains at high temperature [11].

In order to overcome the above shortcomings, some rare earth oxides with low work function are added to pure tungsten electrodes which improve the emission performance of the whole electrode. Commonly used rare earth oxides are La_2O_3 , ThO_2 , Y_2O_3 , CeO_2 and ZrO_2 . Lower the work function of the electrode material easier will be emission of electrons in the gap between electrode and work piece which in turn will improve the arc stability even at low arc voltage, and welding current. The high melting point of the base material permits these cathodes to resist more effectively the high temperatures necessary to the functioning while the low work function of the dopant permits obtaining a high current intensity of electron emission at moderately high temperatures. Various types of electrodes with their characteristics are as follows [12]:

Pure tungsten- It has a high work function, i.e., it takes higher energy to operate which makes it difficult to start and maintain a stable arc. It also has high burn off-rate and thus a shorter service life.

Thoria stabilized- Thoria, although promoting better welding, is low-level, radio-active. Many manufacturers and welders have stopped using it because of the health concerns.

Zirconia stabilized- Zirconia is used for radiographic-quality welding where tungsten contamination must be minimized. In AC application, it balls up easily but has good arc starting and current carrying capacity.

Ceria stabilized- Ceria electrodes are good for orbital tube, pipe, and thin-sheet applications. This formula has low-current capacity but offers low arc ignition and good arc stability.

Lanthana stabilized- These electrodes are a non-toxic and are alternative to thoria-stabilized products. They offer excellent ignition and re-ignition properties

Combination stabilized- Some companies manufacture electrodes with complex oxide stabilization. These advanced non-radioactive formulas combine three oxides with tungsten to produce excellent all-purpose electrodes. They offer long life, repeatable performance, and reliable starting of arc even after high number ignitions. Colour coding is used on some electrodes but this practice is not standardized for all mixes and varies from Europe, Japan, and the United States.



Table 1: Color codes and alloy element contents of tungsten electrode alloys [13]

Classification (as per DIN EN 26 848)	Color	Alloying Element Used	Alloying Oxide	Nominal Content (wt%)
W(WP-00)	Green	-	-	-
WT – 10*)	Yellow	Thorium	ThO ₂	1.0 %
WT – 20*)	Red	Thorium	ThO ₂	2.0 %
WT – 30*)	Purple	Thorium	ThO ₂	3.0 %
WT – 40*)	Orange	Thorium	ThO ₂	4.0 %
WZ – 08	White	Zirconium	ZrO ₂	0.8 %
WC – 20	Grey	Cerium	CeO ₂	2.0 %
WL – 10	Black	Lanthanum	La ₂ O ₃	1.0 %
WL – 15	Gold	Lanthanum	La ₂ O ₃	1.5 %
WL – 20	Blue	Lanthanum	La ₂ O ₃	2.0 %

2.4 Emission of electrons and its mechanism

A welding arc is an electric discharge that is developed due to flow of current from cathode to anode. For initiating the arc and its maintenance, charged particles are needed mostly in the form of ions and electrons. These charged particles in the arc are generated by various mechanisms such as thermal emission, field emission and secondary emission, etc. The Emission of electrons from the cathode depends on work function of its metal or Ionization potential.

1. Work function: It is defined as the energy required to get one electron released from the surface of the material from its metal.
2. Ionization potential: It is another measure of ability of a metal to emit electrons and is defined as energy required per unit charge for removing an electron from an atom.

Metal with low work function or Ionization potential release the electron easily at lower energy level and vice-versa.



2.4.1 Mechanism of emission

- i. **Thermionic Emission:** Thermo-ionic emission is one of the mechanisms through which electrons are emitted and generated in the arc gap. The principal of this mechanism is very simple. Increase in temperature of the metal increases the kinetic energy of the free electrons. As soon as this energy of the free electrons goes beyond a certain limit, electrons are ejected from the metal. But, it happens only at high temperature.
- ii. **Field Emission:** In this approach, high potential difference is maintained between electrode and workpiece so that the development of high strength electromagnetic field helps to pull out the electrons from the surface of the metal. But it is important to have high Potential difference (10^7 V/m) for field emission.
- iii. **Secondary emission:** The generated high velocity electrons already collide with other gaseous molecules on its way which in turn causes decomposition of molecules into ions and electrons that result in further secondary emission.

The effective work function clearly decreases with increase of La_2O_3 content of tungsten electrode (at constant arc current of 100A), which shows the same tendency with the tip temperature as described below in table [14].

Table 2: Change in Tip Temperature and Work function as a function of lanthana content

Electrode type	Tip Temperature ($^{\circ}\text{C}$)	Work function (eV)
Pure W	3788	2.9
W-0.5% La_2O_3	3621	2.3
W-1% La_2O_3	3415	2.3
W-2% La_2O_3	3079	2.0



2.5 Effects due To high temperature on erosion of tungsten electrode in TIG welding

- i. **Resistive Heating:** High electric current passes through the tungsten electrode. The temperature of electrode increases due to resistive heating. As advised by ISO standards current value is restricted as according to diameter of electrodes. This restriction limits the heating to not harmful level for the electrodes except for the tip region where diameter is relatively smaller. This effect is observed in very sharp tip electrodes with a very small tip angle. Florent Simonot had experimentally detected this type of electrode degradation keeping tip angle 30° at current 200A [15].
- ii. **Cooling effect of electrode:** Thermionic emission is a process where thermal energy causes a broadening of the electron distribution such that some higher energy electrons will emit into vacuum [16]. For thermal emission of electrons from electrode (DCEN), energy needed by electrons to jump is equal to its work function from tungsten electrode leads to decrease in its net internal energy, consequently reducing temperature of electrode tip. This effect is called Electron Cooling of Tungsten electrode due to electronic current.
- iii. **Thermal heating due to ions:** Positively charged ions from anode collide at the electrode tip and combine with electrons. Due to this exothermic process, temperature at the tip of the electrode increases.
- iv. **Migration and Evaporation of micro-emitter particles:** In doped electrodes, it is observed that rare earth metal oxides form tungstates or oxytungstates during arc burning which have low melting points and migrate from the low temperature zone to high temperature zone throughout the electrode tip. Migration rate increases considerably with the increase in temperature gradient and depends on melting point of the compounds formed. Because of the lower melting point of compounds formed, La_2O_3 has easier migration and it is continuously fed to the electrode surface. Loss of these oxides due to evaporation at such a high temperature of tip leads to decrease in electron emission and increase in tip temperature [17].



2.6 Erosion of electrodes

During arcing, an increment in the temperature of the electrode due to the combined effect of resistive heating, plasma heating and other heating effects takes place. With the span of time, the temperature of the electrode becomes so high that loss of materials from the tip of the electrode takes place which is called thermal erosion of electrode. And this erosion leads to reduction in electrode life. Electrode life needs to be improved in order to improve the performance of plasma torches due to the essential role of tungsten cathodes as electron emitters.

Some research scholars from Osaka university produced and investigated various types of tungsten-oxide electrodes through comparative study of their characteristics, such a starting performance, electrode consumption, changes in electrode shape due to long term operation, and incompleteness of inert gas shielding and electrode temperature [18]. Also the behaviour of rare earth metal oxides (La_2O_3 , Y_2O_3 , CeO_2 , ZrO_2 , ThO_2 And MgO) has been studied. This study reveals that $\text{W-La}_2\text{O}_3$ electrodes have superior characteristics like high arc pressure, sharp pointed tip and stable microstructures that can be seen in Figure 2.5- Figure 2.7. which strongly depends on behavior of oxides. And, $\text{W-La}_2\text{O}_3$ electrodes have a higher arc pressure, higher emissivity and lower work function followed by W-CeO_2 and W-ThO_2 electrodes. The oxides which has high continuous migration, La_2O_3 , possess a lower work function compared to Y_2O_3 .

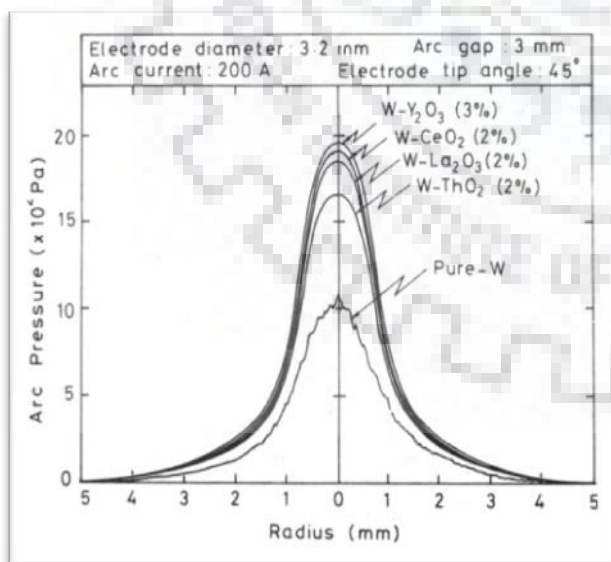


Figure 2.5: Effect of different dopants on Arc Pressure[18]

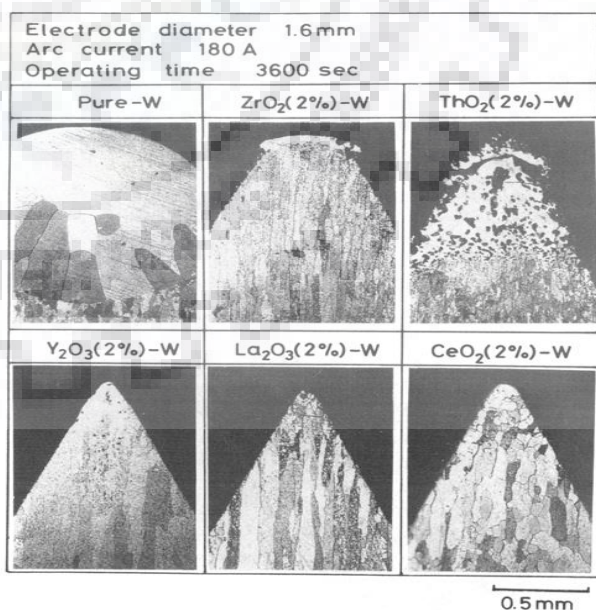


Figure 2.6: Metallurgical microstructure of an electrode cross section after heavy loading[18]



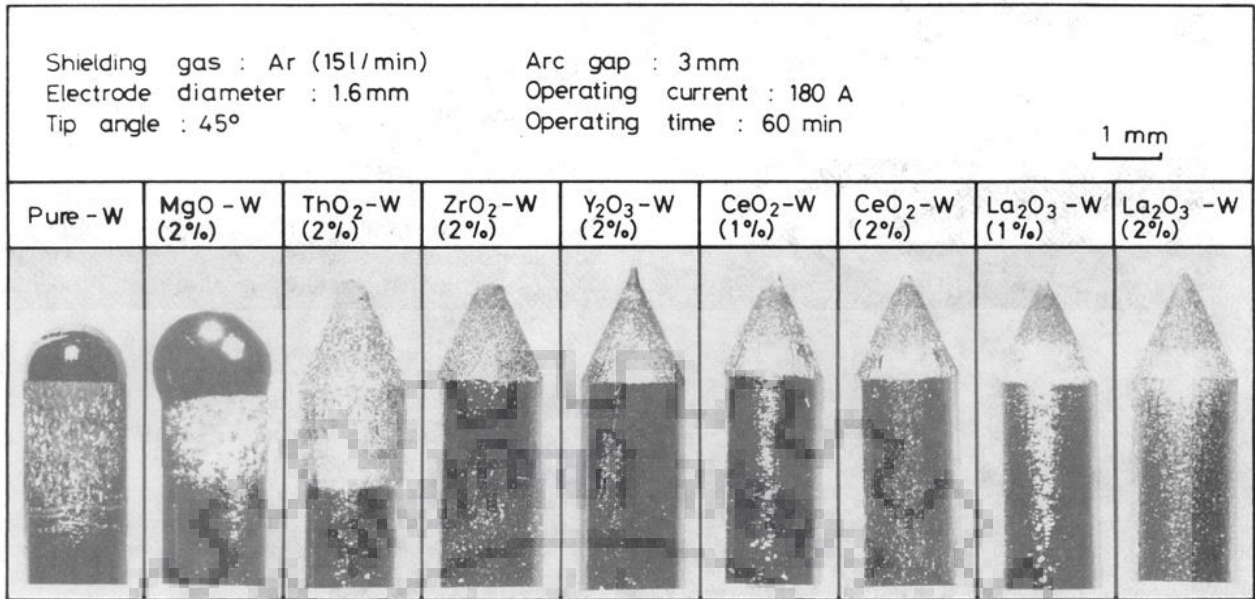


Figure 2.7: Electrode tip Appearance[18]

Koichi Owaga et.al[19] observed the effect of arc current, ambient pressure and electrode diameter on erosion of electrodes doped with 2 wt% of ThO₂, La₂O₃, and Y₂O₃.

The study reveals the same that Lanthanized electrode possess superior characteristics of all the doped electrodes. And erosion in all electrode increases with an increase in ambient pressure and arc current, whereas, with increasing electrode diameter showed decrease in erosion as shown in figure 2.8.and 2.9.

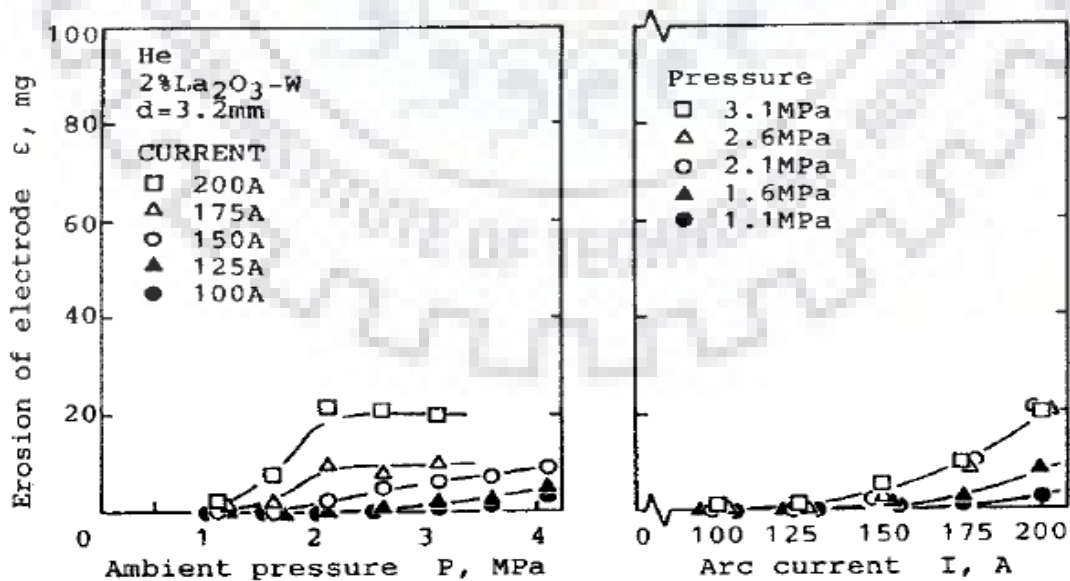


Figure 2.8: Erosion as a function of ambient pressure and arc current[19]

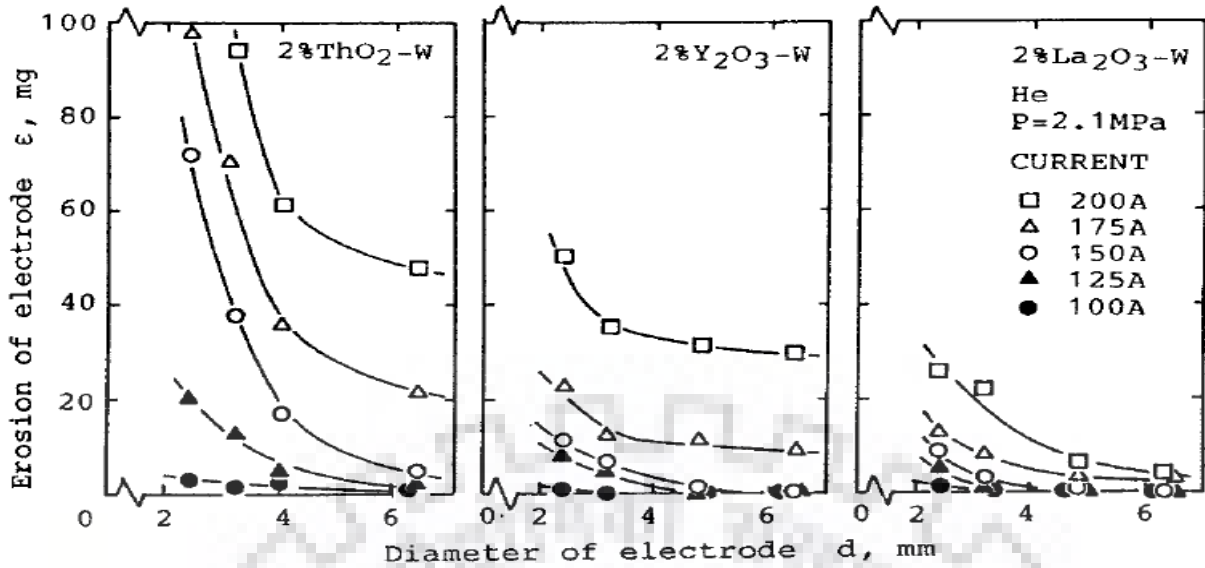


Figure 2.9: Erosion as a function of electrode diameter[19]

Electrodes activated with three combined additions of those oxides were also studied, and it was observed that specially Type R, reflected higher endurance to long time operation than the other single added electrodes as shown in Fig.2.10 - Fig.2.11 [20].

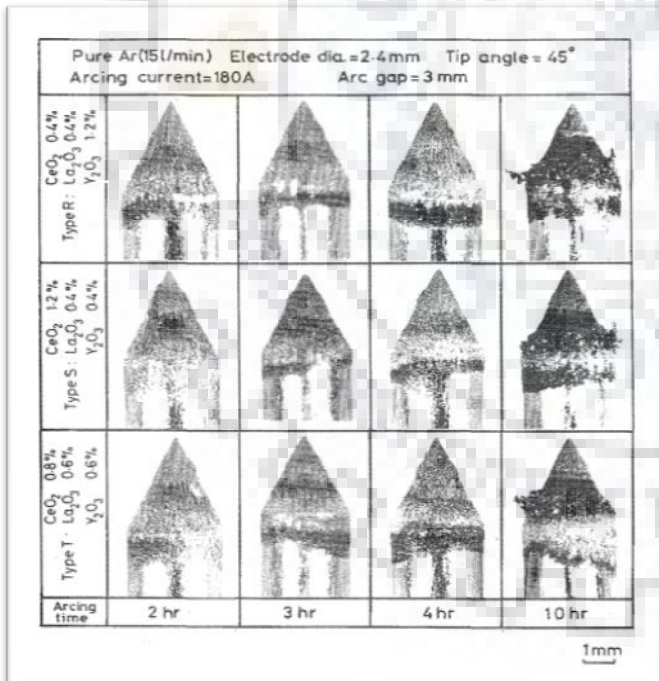


Figure 2.10: Change in electrode tip shape due to long time operation ($\text{La}_2\text{O}_3 + \text{CeO}_2 + \text{Y}_2\text{O}_3 = 2\%$)[20]

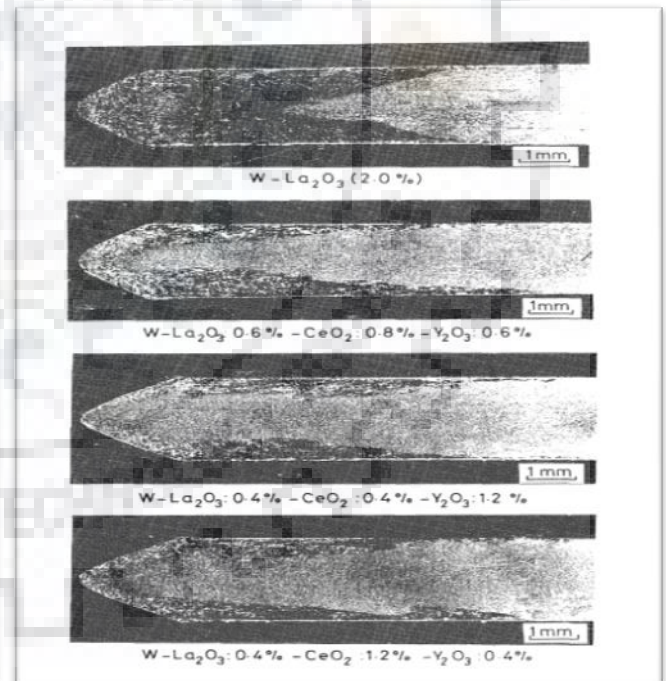


Fig 2.11: Typical macrostructure of tungsten electron activated with combined additives of rare earth metal oxides after 10 hr arcing at 180A A in pure Ar[20].

This is due to the presence of Y_2O_3 and the migration process retardation of La_2O_3 and CeO_2 . The mixing ratio 1:1:3 of $La_2O_3:CeO_2:Y_2O_3$ gave the best balance between arc characteristics, high endurance to long time operation, good stability of oxides and acceptable resistance to rim formation.

To determine the working region with least erosion and also to select the best dopant as per the working regime, erosion in electrodes doped with different rare earth oxides as a function of arc current intensity were also studied by weighing the cathode before and after arcing.[21]. The critical current intensity for 2 wt% lanthanized tungsten is 110 A as shown in Fig. 2.12.

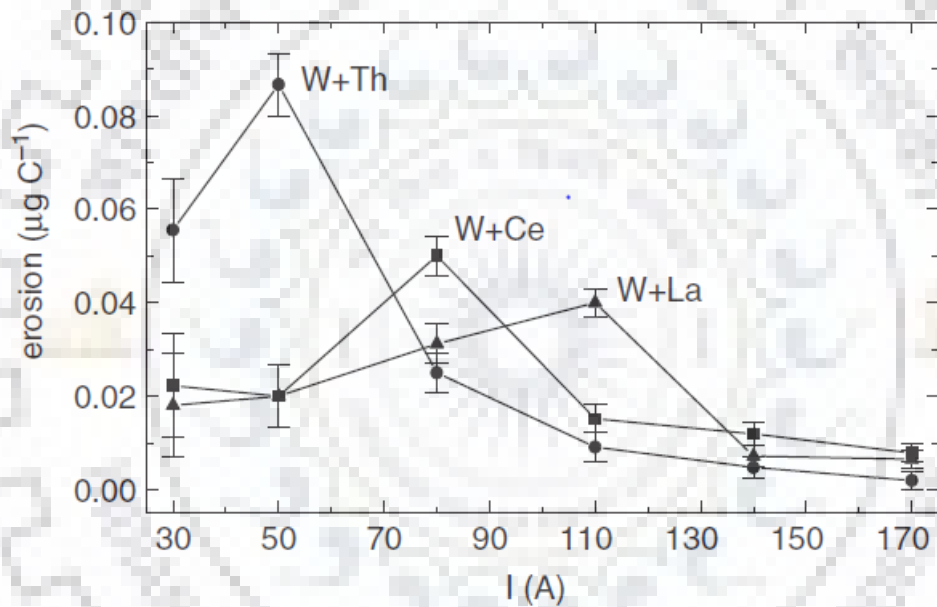


Figure 2.12: Erosion rate on arc current Intensity in conical cathodes. Arcing time = 5 min[21]

Small addition of rhenium in electrode with combination of three rare earth metal oxides can reduce the work function of the material as well as material ablation. Also, rhenium helps in refinement of recrystallized grains that helps in improvement of migration rate of rare earth oxides that increases its stability and provides good welding performance [22].

3. FORMULATION AND PLANNING OF EXPERIMENTAL WORK

3.1 Requirement of the experimental work

From the before mentioned literature, it is clearly observed that during TIG welding, the non-consumable tungsten electrode is getting consumed because of the cumulative effect of various high temperature effects like resistive heating, evaporation/migration of rare-earth metal oxides and electrode cooling which is causing erosion in the electrode and reducing its life. Moreover, it is still not well understood how the rare earth particles influences erosion mechanism and working temperature of the electrode. Thus, for developing certain methods to improve the life of electrodes it is very important to study the mechanism of erosion in a more detailed manner.

For TIG welding, the performance of the electrode is dependent on the tip geometry as it influences current loads and arc pressure [20]. Arcing for higher time changes the shape of electrode tip and makes it blunt causing increase in the tip angle and spreading of the arc. Higher the tip angles, lower the arc pressure that leads to lower weld penetration which effects soundness and quality of weld. And the performance of the electrode is affected by thermal erosion of electrode tip due to melting/evaporation at high temperature. Also changing the eroded electrode with the fresh one adds to the cost and loss in production time on the work table.

Due to high melting point, pure tungsten is used as TIG electrode. It has a very high work function thus a high working temperature which reduces thermionic emission from the cathode surface, so fraction of ionic current to total current increases. This leads to intensive heating due to recombination of ions with electrons at the tip surface and causing melting/evaporation of electrodes. To overcome these shortcomings La_2O_3 particles are implemented in tungsten which lowered the work function and improves emission efficiency.

The present experimental work focuses on to study the extent of erosion and its mechanisms in pure tungsten and 1.5% La_2O_3 doped tungsten electrodes at different arcing time weld cycles and to make an image model in order to illustrate these mechanism and answer the following questions.

1. How high temperature diffusions leads to local change in concentration of lanthana by migration and evaporation process.

2. What are all new phases forming and how these phases are varying with increase in arcing time.
3. How grain growth is occurring in pure and La doped electrodes and effecting migrating process.

For that it is important to analyze the concentration of the dopant from the centre of the electrode towards the electrode tip and its surface at different regions and the type of phases forming that will give us information about extent of diffusion and whether the phases mentioned by Osaka researchers are forming or not. The extent of erosion, grain growth and grain size will be studied by using optical microscope and Scanning electron microscopy. Elemental analysis will be done by Energy Dispersive X-Ray Spectroscopy (EDX) Technique. Alongside X-Ray Diffraction Analysis (XRD) determines the phases forming in electrode tip and how their fraction is changing w.r.t different arcing time. The resultant data will be used to explain erosion of tip and to making an image model depicting erosion mechanism.



3.2 Planning of the experimental work

For a tungsten electrode, Current and time are governing independent parameters for its erosion (keeping metallurgy, cooling capacity of welding torch constant). So Tip erosion can be study by changing these parameters only. Arcing is done on pure W and doped La_2O_3 W electrodes for different arcing times.

Table 3:Electrodes with different arcing time and corresponding weld cycles

Total arcing time duration (Min)	Pure tungsten electrodes	1.5% La_2O_3 tungsten electrodes	No of weld cycles (N)
0	W _{ref}	W _{La_{ref}}	0
5	W ₀₅	W _{La_05}	1
10	W ₁₀	W _{La_10}	2
15	W ₁₅	W _{La_15}	3
30	W ₃₀	W _{La_30}	6
45	W ₄₅	W _{La_45}	8
60	W ₆₀	W _{La_60}	12
75	W ₇₅	W _{La_75}	15
90	W ₉₀	W _{La_90}	18
105	W ₁₀₅	W _{La_105}	21
120	W ₁₂₀	W _{La_120}	24

In real Industry application, the arcing process is not continuous due to changing of filler wire and changing of weld samples. Also, during repeated start and shut down processes, there will be tip melting, solidification, recrystallization processes, which can effect performance of electrode due to grain coarsening.



Temperature dependant diffusion may also effect the concentration of La doped particles within grain boundaries.

So in order to simulate the actual working conditions as in industry, the arcing process consisted of repeated start and shutdown process at different arcing time for different weld cycle. Following steps are planned to depict the influence of rare earth metal oxides in tungsten electrodes as shown in Fig. 3.1.

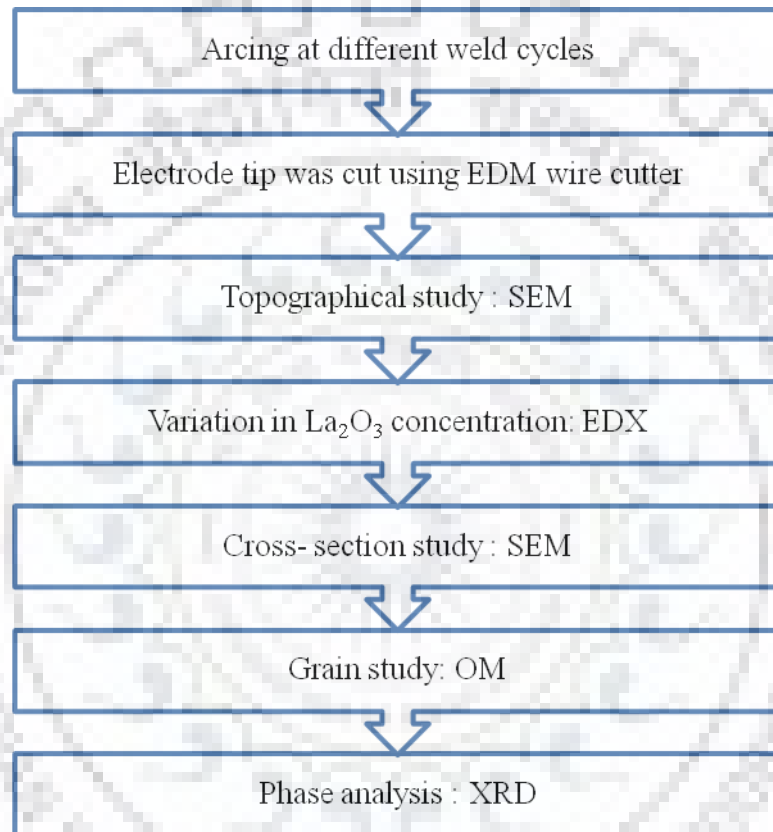


Figure 3.1: Steps followed for evaluating behavior of rare earth oxides

4. DESIGN OF EXPERIMENTAL WORK

4.1 Equipment for Arcing-

A TIG welding torch, welding power machine, cooling system for electrode and copper base metal was used for arcing as shown in below figure . As copper have excellent heat conductivity it was used for designing a water cooled anode point, which can sustain high temperature during static arcing. The arcing was performed with an ABITIG 300W (Binzil) TIG welding Torch. The Torch is set in a movable clamp, above the water cooled copper plate. Tungsten Electrodes DIN EN ISO 6468, diameter of 3.2mm, length 17.5 cm are used in this torch.

The arc is established between the copper plate and the electrode tip without the melting of copper plate. The gas flow rate can be adjusted between 0L/min to 20L/min with its control panel. The torch can be moved horizontally over the copper plate, but for this experimental work it was kept stationary during the arcing. Arc length is directly related to the arc voltage



Figure 4.1 : View of welding machine used for arcing



and arc temperature, so for the whole experimental work ,it was kept constant (3mm) to avoid any error.

Table 4:Welding parameters for arcing

Shielding Gas	Argon
Flow rate	12 L/min
Pre Gas flow time	5 sec
Post Gas flow time	20 sec
Electrode Parameters	
Electrode type	1.5% La ₂ O ₃ Tungsten electrode
Electrode Diameter	3.2 mm
Electrode Tip angle	60°
Total length of Electrode	17.5 cm
Coolant Medium of torch and work piece	Water
Length of electrode outside of Copper collet	27 mm
Current Specification	
Welding Current Levels	200A (DCEN)
Voltage level	12-13 Volt, Variable
Arc length	3mm
Step up time	1.5 sec
Starting current	20 % of fixed current
Step down time	1 sec

As discussed above the images of electrode tip will be used for comparing the erosion process at different arcing time and fixed current of 200A.





Fig 4.2 : La Doped Electrode tips after welding for different arcing time

4.2 Tip surface topography examination by optical microscopy and scanning electron microscopy

The microstructure of the used electrode's tip surface as well as cross-section were taken by **Jeol JSM 6300 SEM** whose specifications are as follow:

Magnification: 10X-300000X

Type of electron gun: Tungsten Thermionic gun

Accelerating Voltage: 5-30 kV

Resolving Power: 11nm

Vacuum: 10^4 Pa

The following characteristics were analysed:

- Appearance and stability of electrode tip
- Grain growth
- Surface morphology
- Whether zones are forming or not and how these zones are varying w.r.t arcing time
- Electrode tips were cut axially and again investigated by SEM and EDX.



4.3 Elemental analysis of tip surface by EDX

As per diagram, EDX line scan and mapping of different portion were done by **EDX Quantax 200 (High Speed Detector)**. Variation in La_2O_3 content in different regions (tip to bulk) was investigated which is helpful for qualitative study of Lanthana and gives us idea about migration and evaporation process.

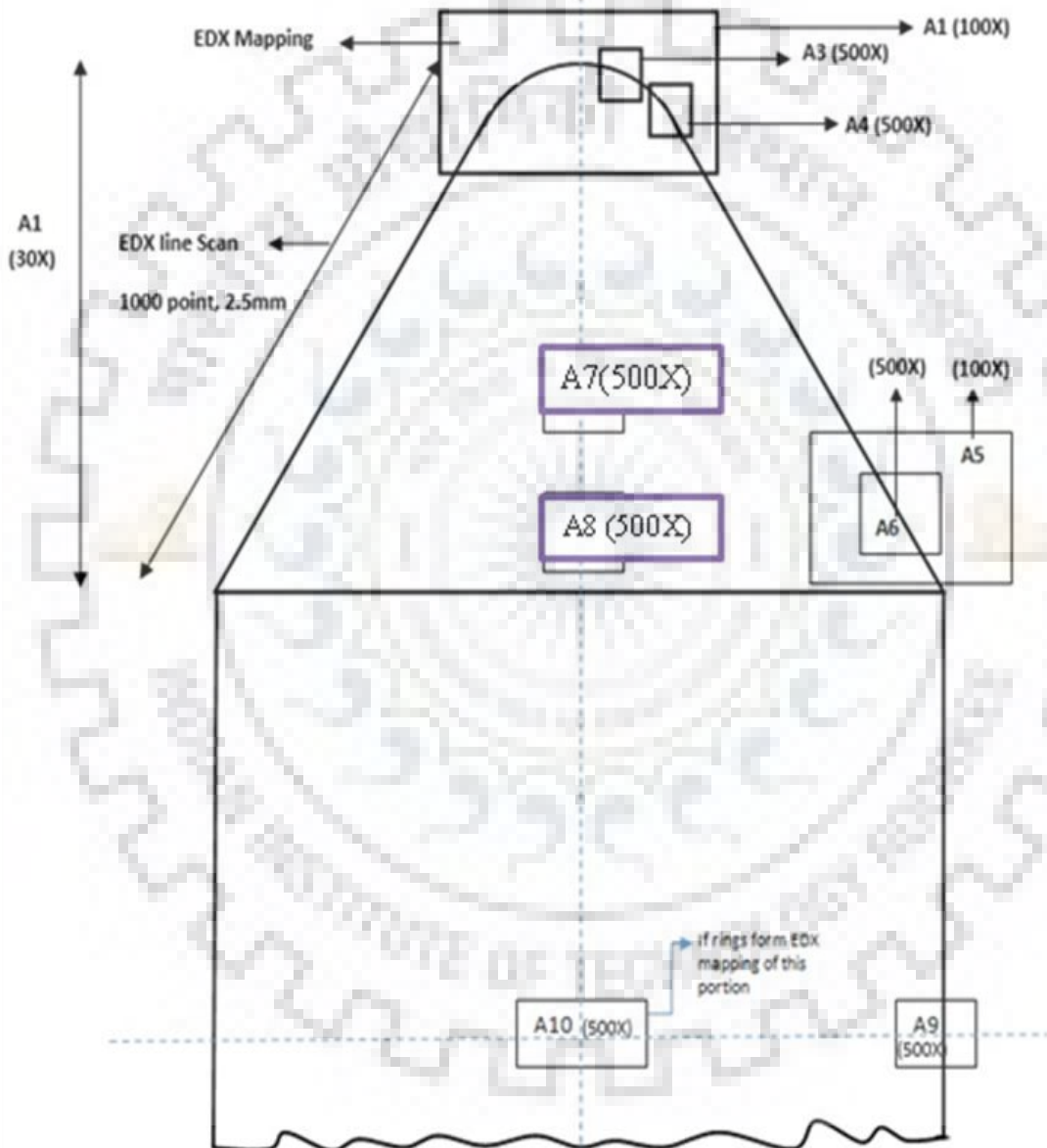


Fig. 4.3 : Schematic plan for SEM and EDX experiment

4.4 X-ray diffraction analysis

Electrode tips were cut along the length using a Well diamond wire saw model 4240 fitted with 0.22 mm diameter diamond coated wire (type A64). Wire saw allows for very slow cutting speeds, which does not heat up the sample, thereby making sure there is no surface oxidation or effect on the microstructure.

X-ray diffraction measurements were performed in a PANalytical diffractometer in the Bragg-Brentano geometry fitted with a X'Celerator detector using a Co $K_{\alpha 1}$ radiation source ($\lambda = 1.7890 \text{ \AA}$) attached to a monochromator. The diffractometer was also equipped with a sample spinner PW 3064 and an automatic sample changer PW3065.

The half cut electrode samples were fixed using an amorphous glue on a single crystalline Si plate with orientation such that it does not give a peak in the measurement. A 3 mm x 3 mm spot size was focused on the tip area, to get information only from the tip.



5. RESULTS AND DISCUSSION

5.1 Stability/durability of the electrode tip geometry

Under the thermionic influence of the electrode work conditions, the tip geometry and surface structure change. In Fig. 5.1, 5.2 and 5.3, a comparative selection of pure tungsten and Lanthanum doped electrode tip surface and geometry is shown. All presented electrodes were working under pure Argon gas shielding with 200A current and a cycle time of upto 120 minutes. It is apparent from the figure below that:

1. Out of the two types of electrodes investigated, W-La₂O₃ electrode retained its pointed tip for high weld cycles and showed higher resistance to erosion. This pointed tip suggests that tip geometry is maintained even after 18 weld cycles, playing a vital role in the performance of electrode.
2. In case of the pure tungsten electrode, the formerly sharp tip was severely melted and blunted while for La doped ones, the electrode tip showed no severe melting but slight and increasing blunting. Tip geometry in pure W electrodes shows strong distortions just after 3 weld cycles, displaying shiny surface on the electrode tips that indicates a melting. This erosion increased as the number of weld cycles were increased.
3. During arcing for 24 weld cycles i.e., 120 minutes, erosion was so high that pure tungsten electrode tip got melted completely.

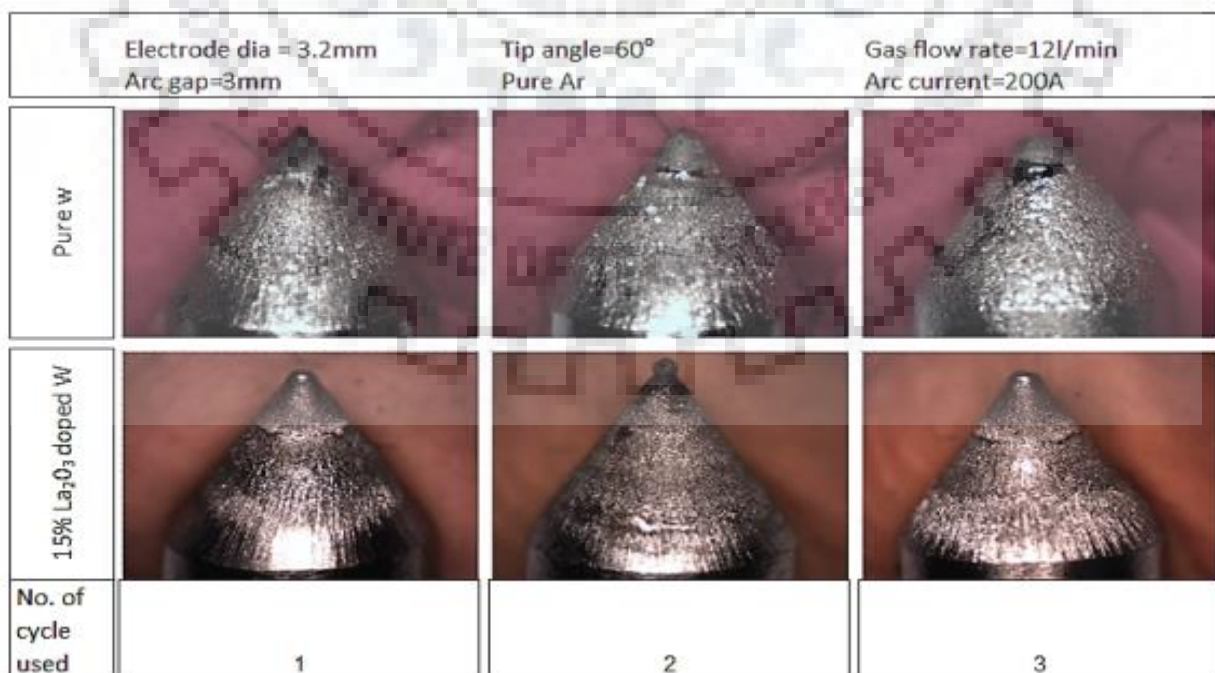


Figure 5.1: Electrode tip appearance after 1, 2 and 3 performing weld cycles






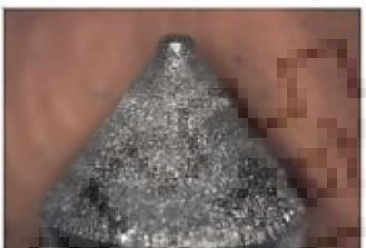


	Electrode dia = 3.2mm Arc gap=3mm	Tip angle=60° Pure Ar	Gas flow rate=12l/min Arc current=200A
Pure W			
15% La ₂ O ₃ doped W			
No. of cycle used	6	9	12

Figure 5.2: Electrode tip appearance after 6, 9 and 12 weld cycles




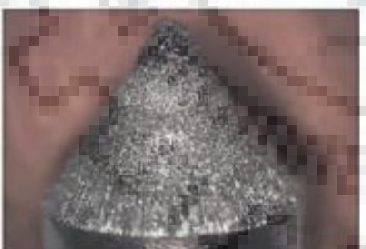
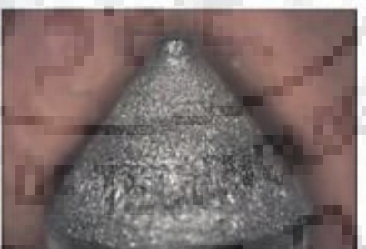

	Electrode dia = 3.2mm Arc gap=3mm	Tip angle=60° Pure Ar	Gas flow rate=12l/min Arc current=200A
Pure W			
15% La ₂ O ₃ doped W			
No. of cycle used	15	18	21

Figure 5.3: Electrode tip appearance after 15, 18 and 21 weld cycles

5.2 Scanning electron microscopy and EDX analysis of electrode tips

5.2.1 Scanning electron Microscopy of La₂O₃ doped Tungsten electrodes

For the topographical study of the electrode tips, SEM images and EDX mapping/line scans were taken from different regions of electrode tip as described earlier in design of experimental work. Fig. 5.4 represents La₂O₃ doped electrode tip zones with different characteristics after arcing.

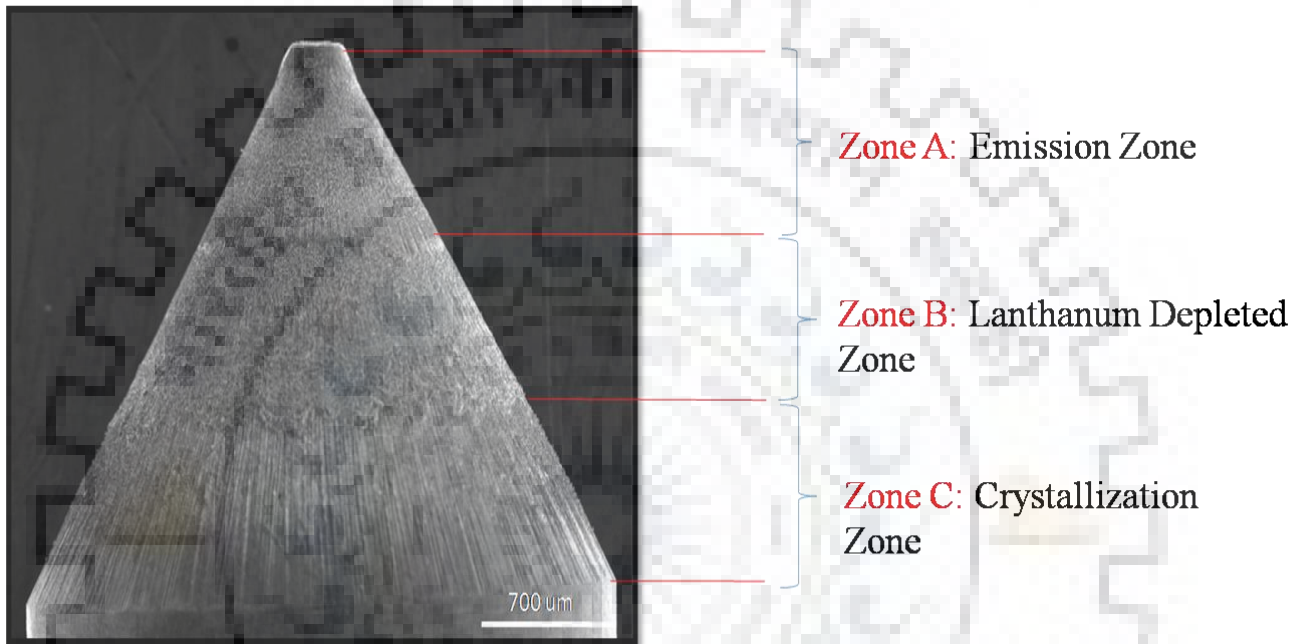


Figure 5.4: Characteristics zones observed in La electrode tip surface in SEM

On the basis of topography of the electrode tip surface, various zones with different characteristics and morphological appearance have been observed. Zone A is the topmost part of the electrode tip where emission takes place is named as emission zone.

Studying the morphology of zone A, it can be noticed that a large number of small, needle like tips are present on a melted layer of tungsten surface, which acts as a source of thermo-ionic emission of electrons

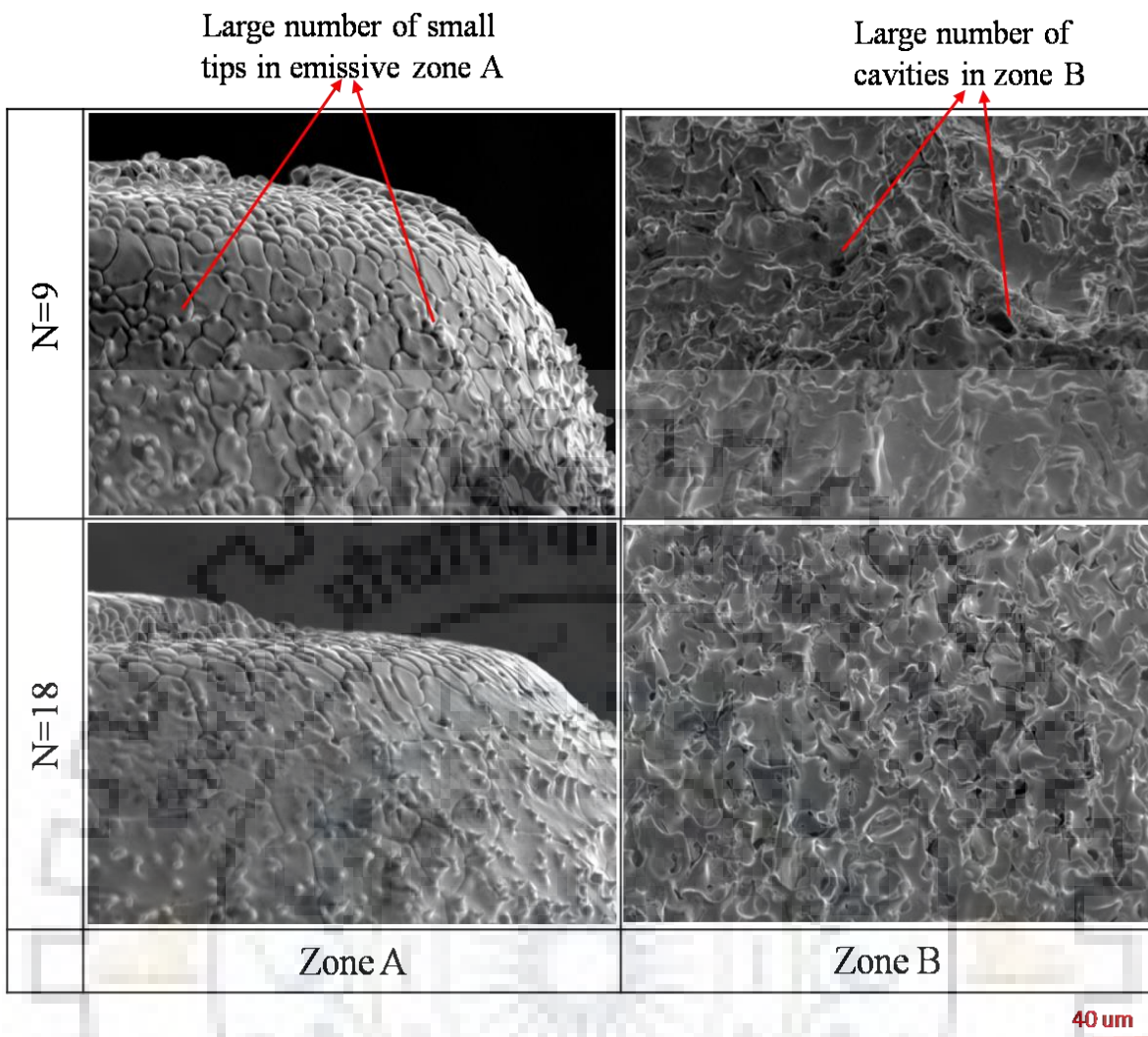


Figure 5.5(a): Microstructural View of Zone A and B after N=9 and 18

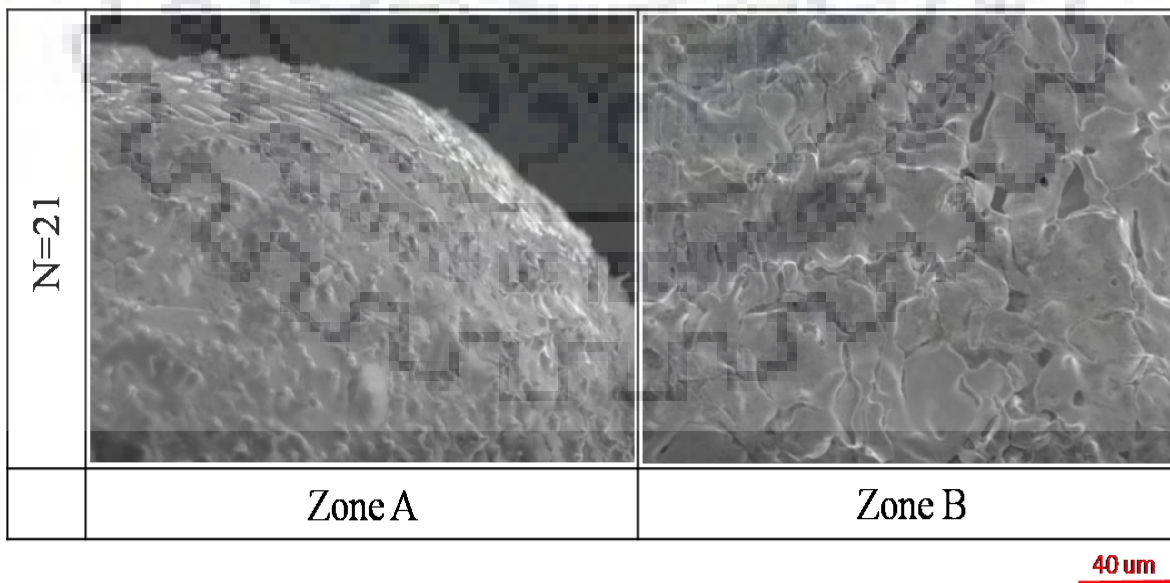


Figure 5.5(b): Microstructural View of Zone A and B after N=21



The magnified view of zone A in Fig. 5.5(a) and 5.5(b) reveals that large number of tips are uniformly distributed across the boiling surface of tungsten which reveals emission is uniform in zone A. In addition to the general surface topology, there are visual lines of grain boundaries, especially in the “pin” area detectable.

The EDX mapping shown in Fig. 5.6(a) and Fig. 5.6(b) indicates an unequal concentration of La particles in Zone A. This reveals that the migration rate of La particles is yet higher than evaporation rate. Interesting to notice is the concentration of at the centre of the formed pin, indicating a migration of La_2O_3 longitudinal from the electrode core to the tip.

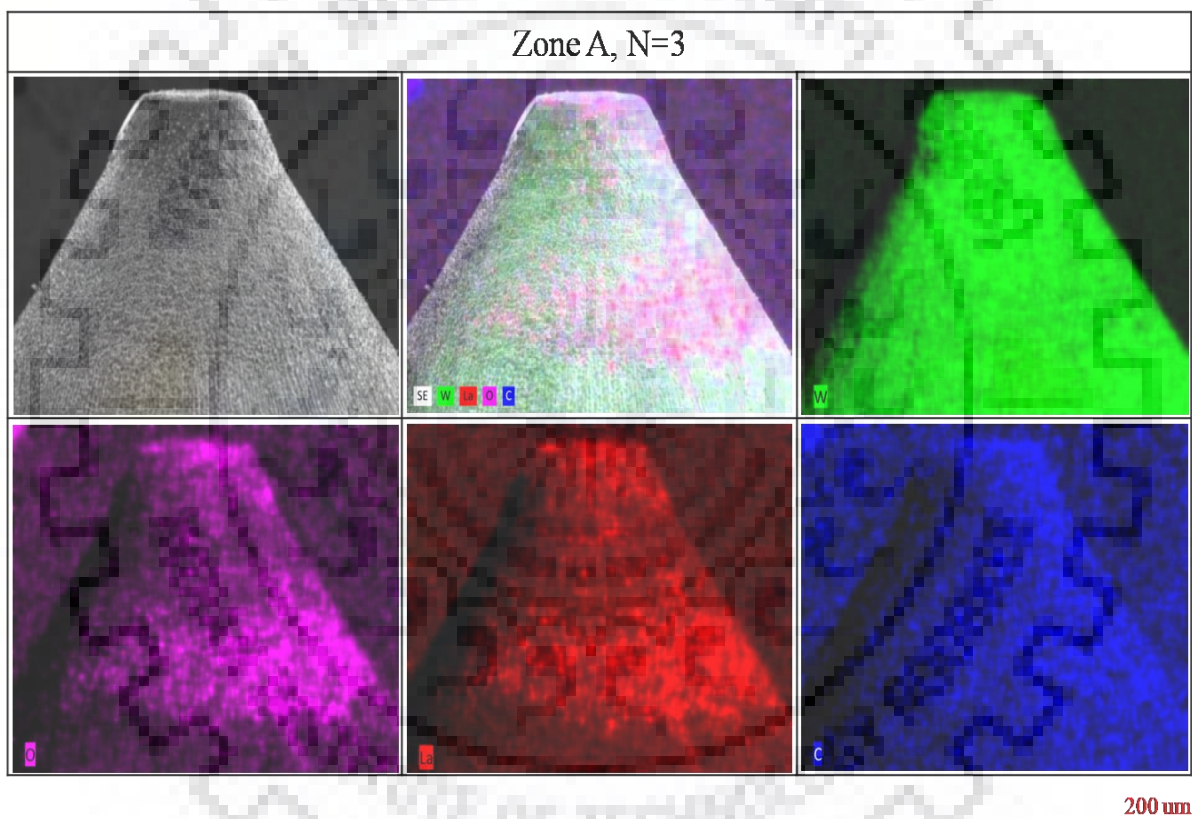


Figure 5.6(a) : EDX mapping of zone A after N=3

In the magnified view of zone B, there is no sign of any significant formation of electron emissive tips detectable. A surface with a number of cavities has been observed here. It is believed that the combined effect of arc plasma heating and resistive heating made this zone the highest evaporation zone. Absence of La particles in this zone represents that the evaporation rate of La particles are higher than migration rate.

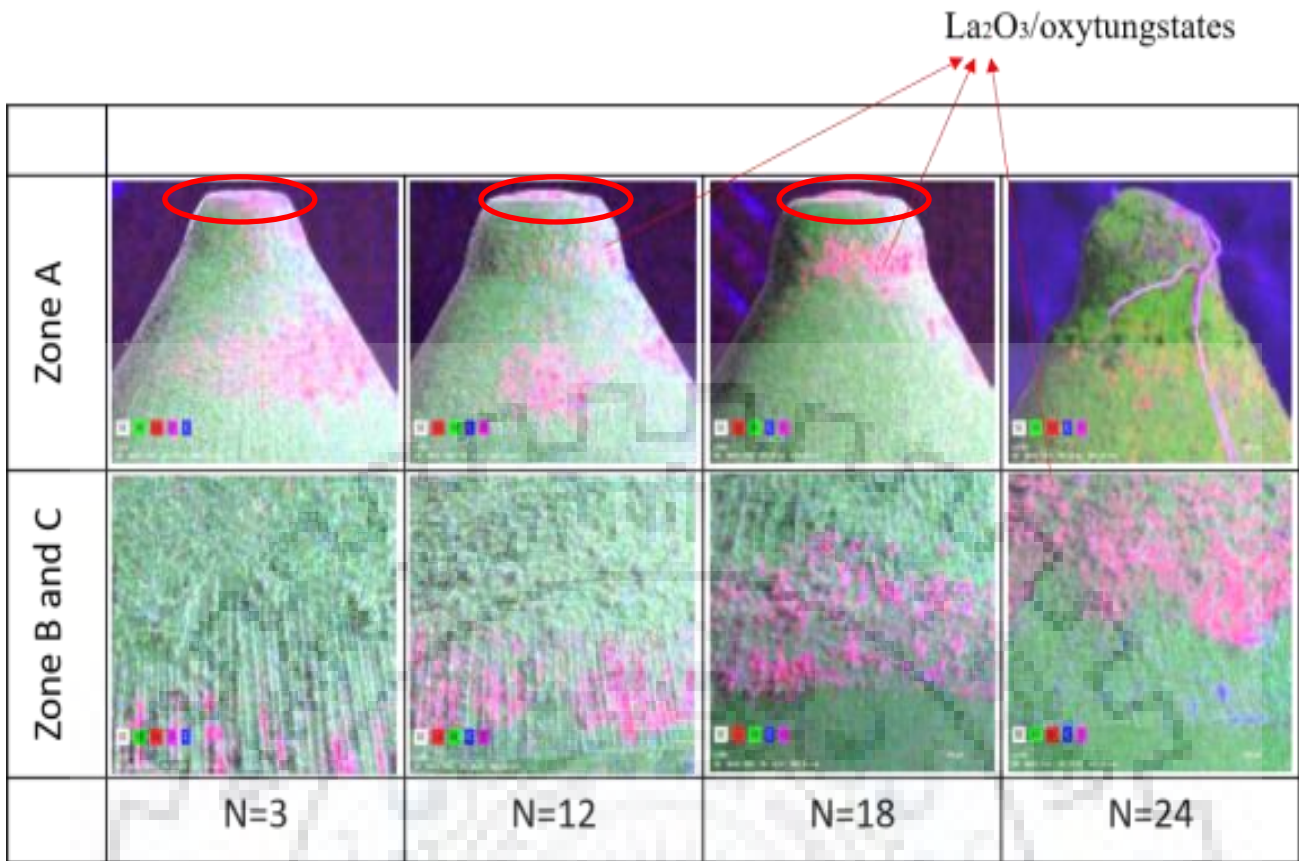


Figure 5.6(b) : EDX analysis of different zones observed in La_2O_3 doped electrode tips

Fig. 5.7 also shows zone C whose surface appearance mainly rough with no signs of melting surface. It has been observed that crystallization of pure tungsten is taking place.

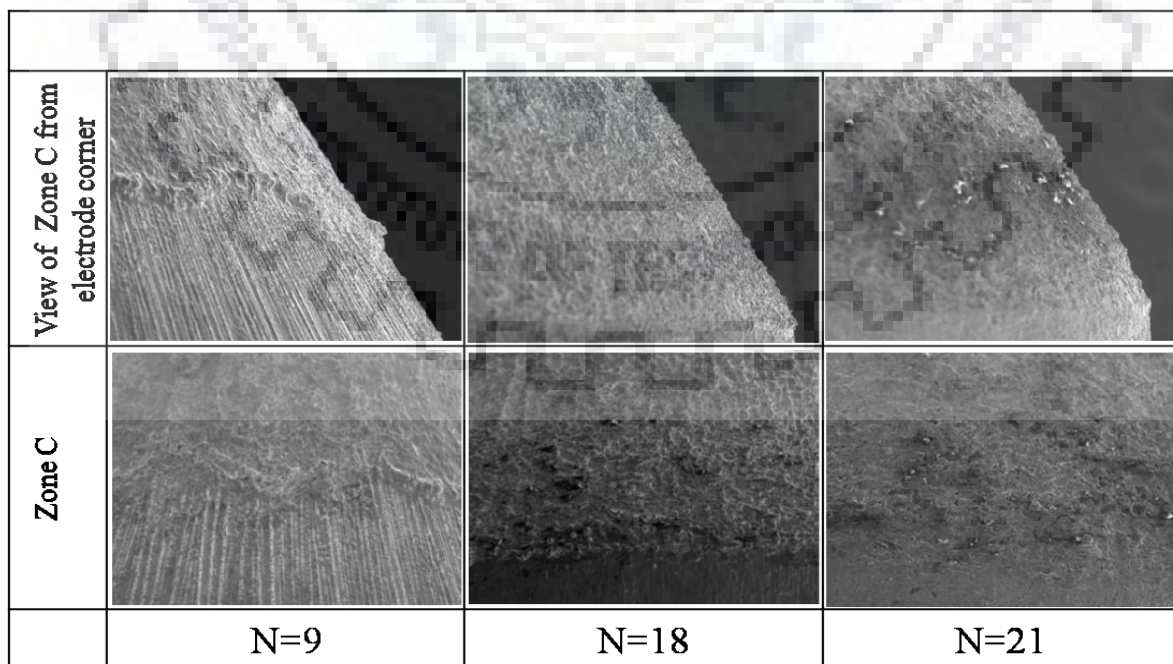


Figure 5.7: Microstructure of crystallization zone C

200 um



It can lead to the assumption that evaporated tungsten from the zone A is depositing in this region of the electrode. Interestingly wise this crystallization takes place mainly along the peak topology of the yet present grinding structure.

The effect of arc heat content and resistive heating is time dependent. As this part is less effected by the arc heating and resistive heating during initial weld cycles, it is considered that this zone has the lowest temperature in comparison to other zones. The Presence of La particles on surface of zone C revealed that migration rate is higher than evaporation rate.

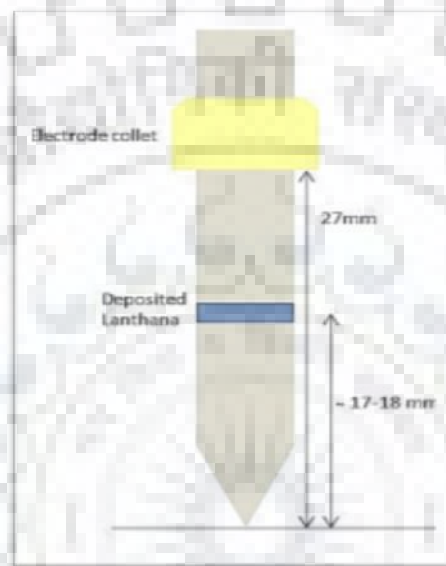


Figure 5.8: Formation of La deposit ring on the upper cylindrical part of electrode

It is also found that a deposition ring has been formed on the upper cylindrical part of the electrode in La doped electrodes as shown in Fig. 5.8. EDX mapping of this ring shows presence of La and O in this region which clearly reveals that La particles which were evaporated from zone A and B is depositing here. This ring is observed for all La_2O_3 doped electrodes except after 1 and 2 weld cycles. Also, thickness and porosity of these rings are increasing with each performing weld cycle as shown in Fig. 5.9(a) and 5.9(b).

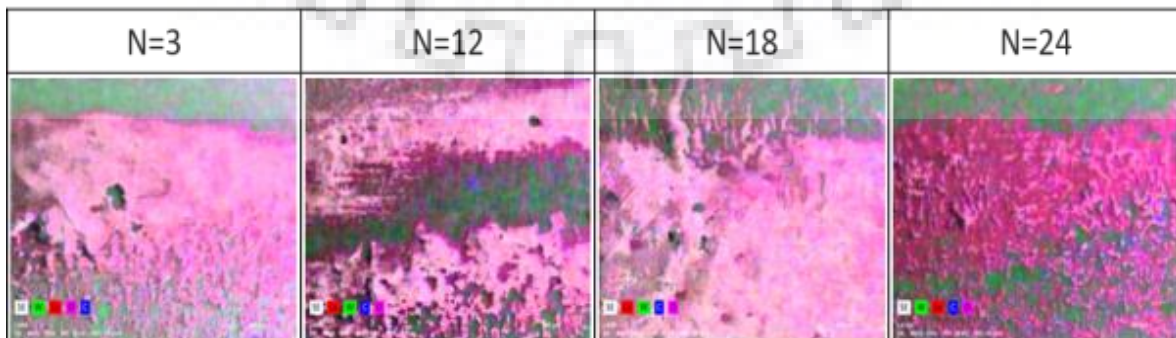


Figure 5.9(a): EDX analysis of ring formed on the cylindrical part

Presence of La and O in upper part of electrode, N=3

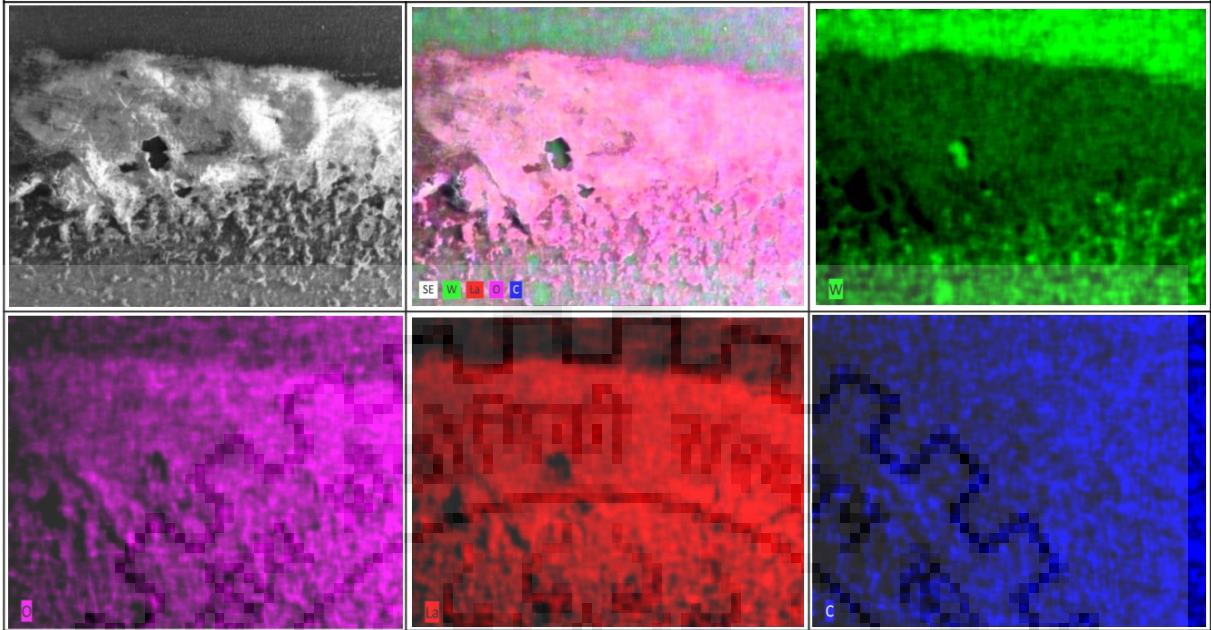


Figure 5.9(b): EDX mapping of La deposit ring on the upper cylindrical part of electrode

5.2.2 Scanning electron microscopy of pure Tungsten electrodes

SEM micrographs of pure tungsten electrode tip after 2 weld cycles is shown in the below Fig. 5.10. There is not any formation of characteristic zones, unlike observed with the La_2O_3 doped electrodes, after initial 2 weld cycles i.e. up to 10 minutes arcing.

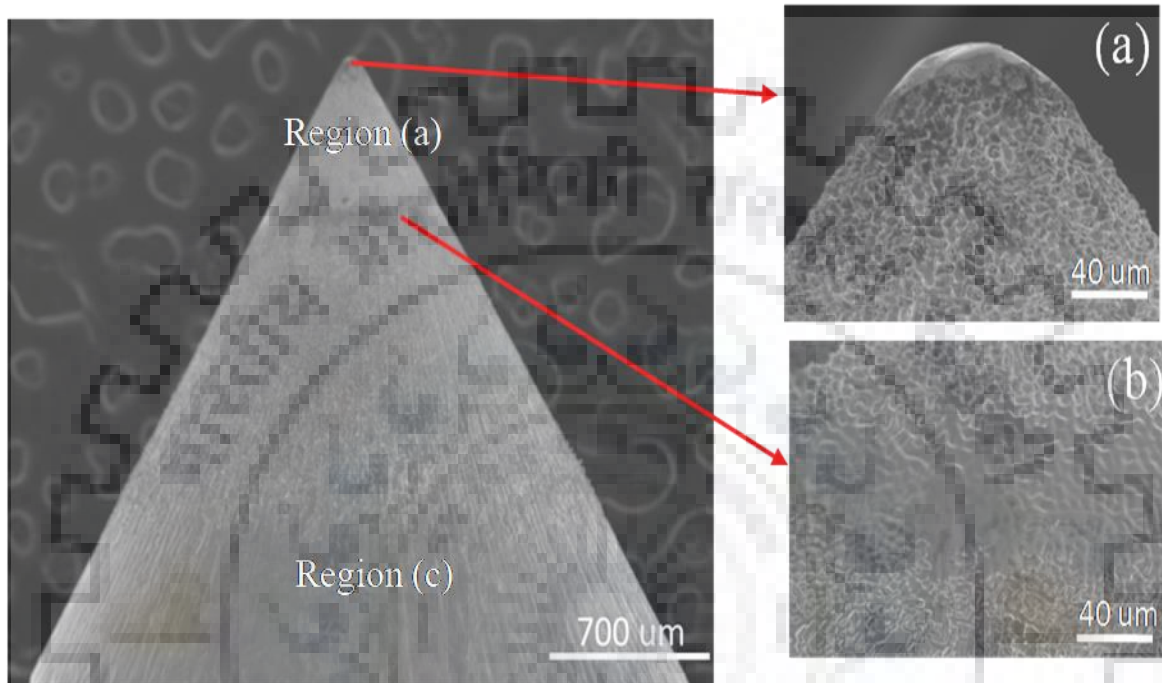


Figure 5.10: Magnified view of different regions in pure tungsten electrode after 10 minutes of arcing

In Fig. 5.10, a re-melted region has been observed at the tip which is shown in (a). Due to the high temperature, the bulges of sputtering shape is formed on the surface of the electrode under the bombardment of positive ions.

A melted ring has been observed in (b) which is due to effect of plasma heating and very high resistive heating. With increase in weld cycles there is not much difference in morphology on the surface of pure tungsten electrode.

After 30 minutes of arcing, no different regions are detected. .With increased time of duty, the working temperature of the electrode is reaching melting temperature so that the erosion is taking place at a very fast rate by melting and evaporation processes and electrode tip is getting shortened as shown in below Fig. 5.11.

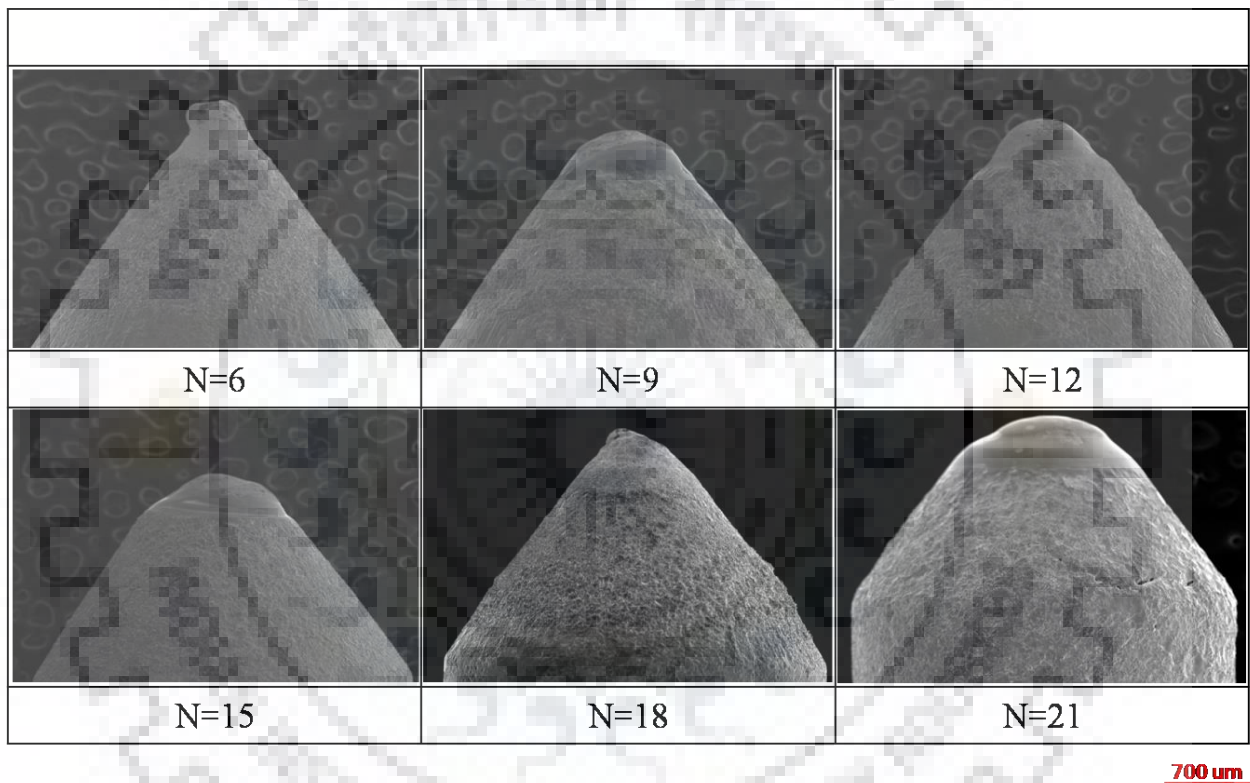
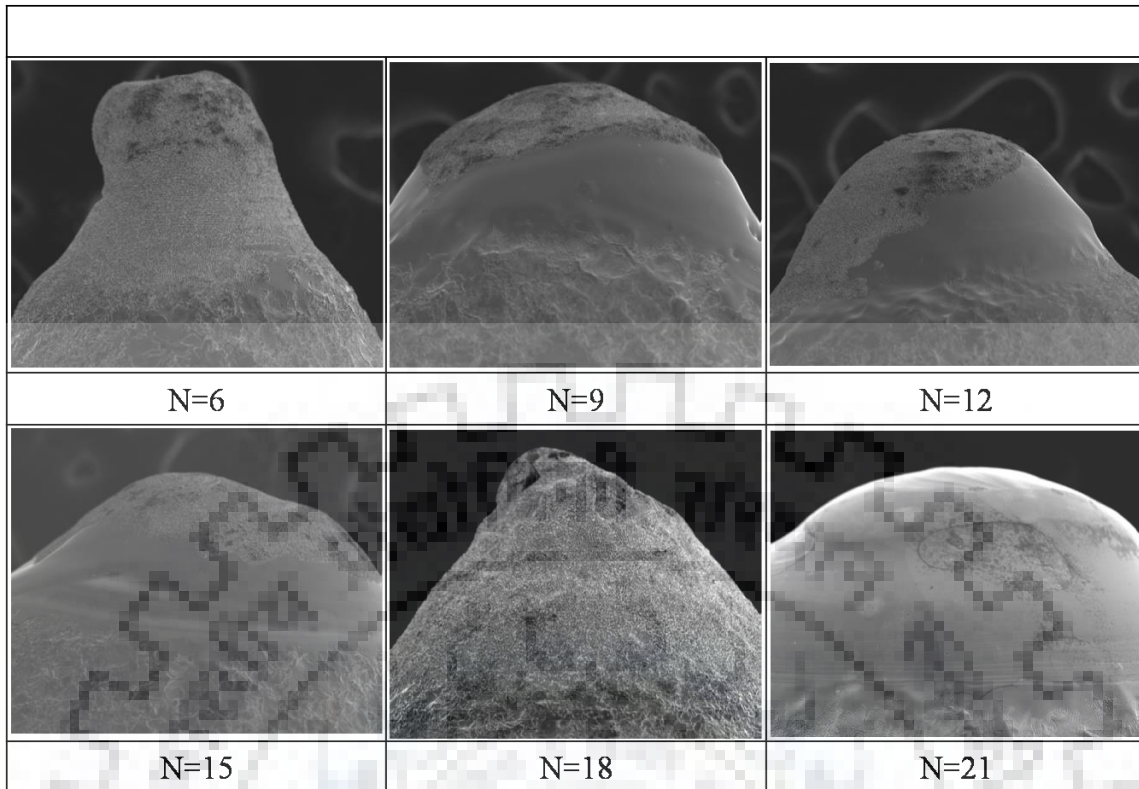


Figure 5.11: Pure tungsten electrode tips under SEM after arcing for different weld cycles

With each performed weld cycle, the emission zone area is increasing of the electrode tip and melting takes place exactly at the tip.

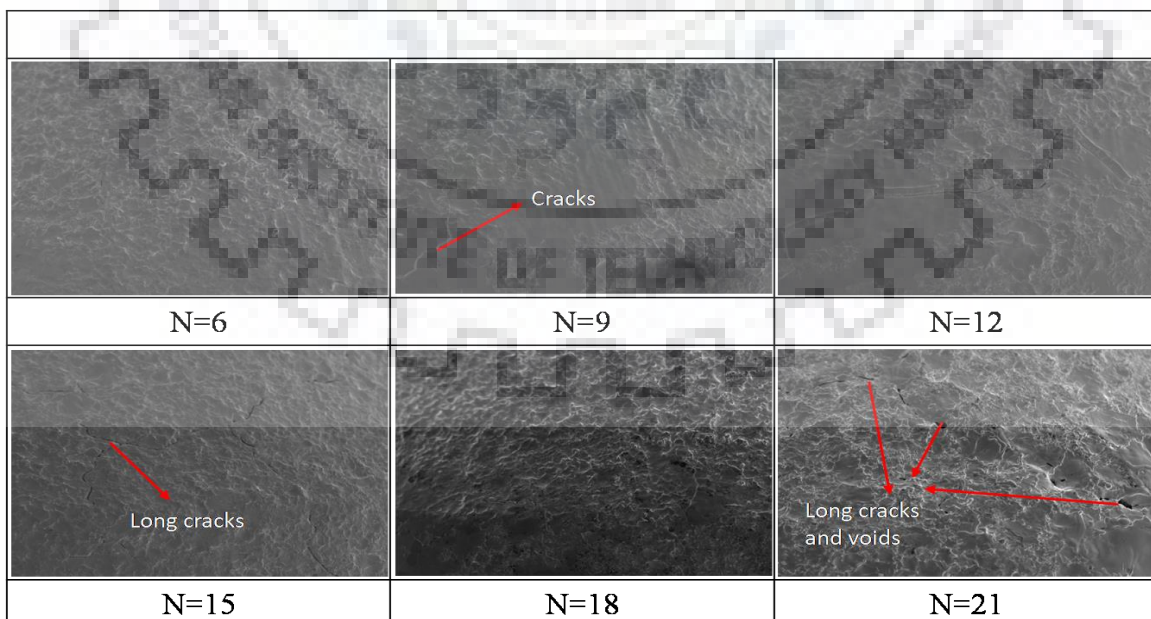
It clearly suggests that, when the arcing was done for longer time, more and more melting as well as very high evaporation of tungsten from the electrode tip is taking place and led to higher erosion of the tip as shown in Fig. 5.12. Because after heavy duty, temperature of the whole electrode tip got increased even up to cylindrical part.



200 um

Figure 5.12: Magnified view of Region (a) of electrode tip

Also, at higher weld cycles of 9, it is clearly observed that in Region (c), electrode surface is melted up to cylindrical part of the electrode as shown in Fig. 5.13. This suggests that the surface temperature of electrode tip becomes very high and electrode tip is deteriorating fast.



200 um

Figure 5.13: Magnified side view of Region (c) in electrode tip after different weld cycles(N)



Fig. 5.14 shows the magnified view of Region (c), which reveals inter granular cracks at the surface of the electrode tip. These cracks are growing with each performing weld cycles and forming cavities/voids at higher weld cycles. It may be because of the expansion and contraction phenomena occurred during switch on and switch off of an arc which causes stress concentration in the electrode tip and led to initiation of cracks.

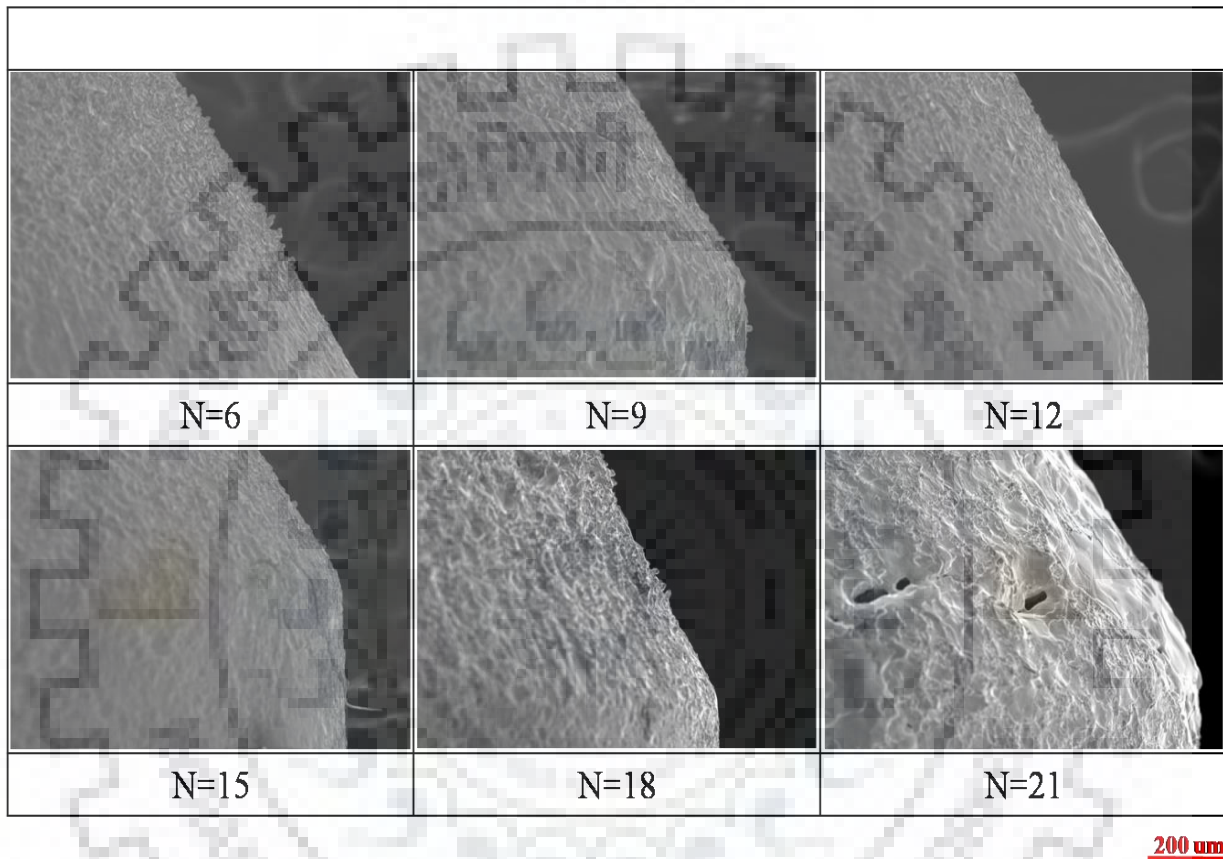


Figure 5.14: Magnified view of Region (c) after different weld cycles(N)



5.3 Cross sectional study of pure W electrode tips

5.3.1 Optical microscopy of electrode tip cross section

To investigate changes in the inner electrode structure, cross sections of the electrode tip area were prepared and reviewed with Optical Microscopy. For the visualization of the metallurgical microstructures the samples were prepared by polishing and following etching with Murakami-solution (100ml water + 10gram NaOH + 10gram $K_3Fe(CN)_6$). For all samples, optical microscope images of the microstructures in region A and B, as shown in Fig. 5.15, were taken.



Figure 5.15: Region on polished electrode tip cross section for optical microscopy

No of weld Cycles	Pure W Electrode Arc Current 200A	
Reference unused		
2		
	Region 1	Region 2

1 mm

Figure 5.16: Metallurgical microstructures of an electrode cross section of unused electrode and after 2 weld cycles



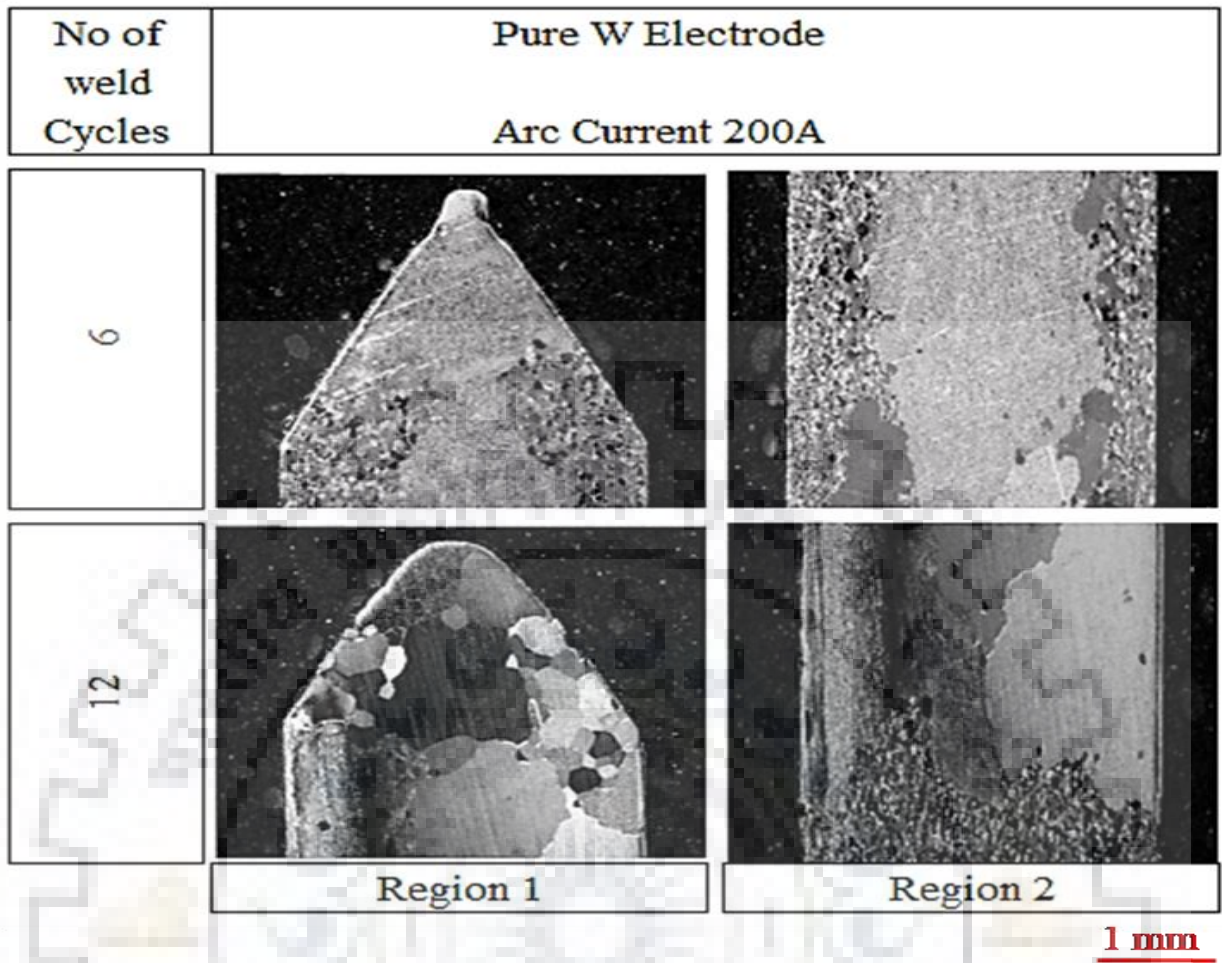


Figure 5.17: Metallurgical microstructures of an electrode cross section after 6 and 12 weld cycles

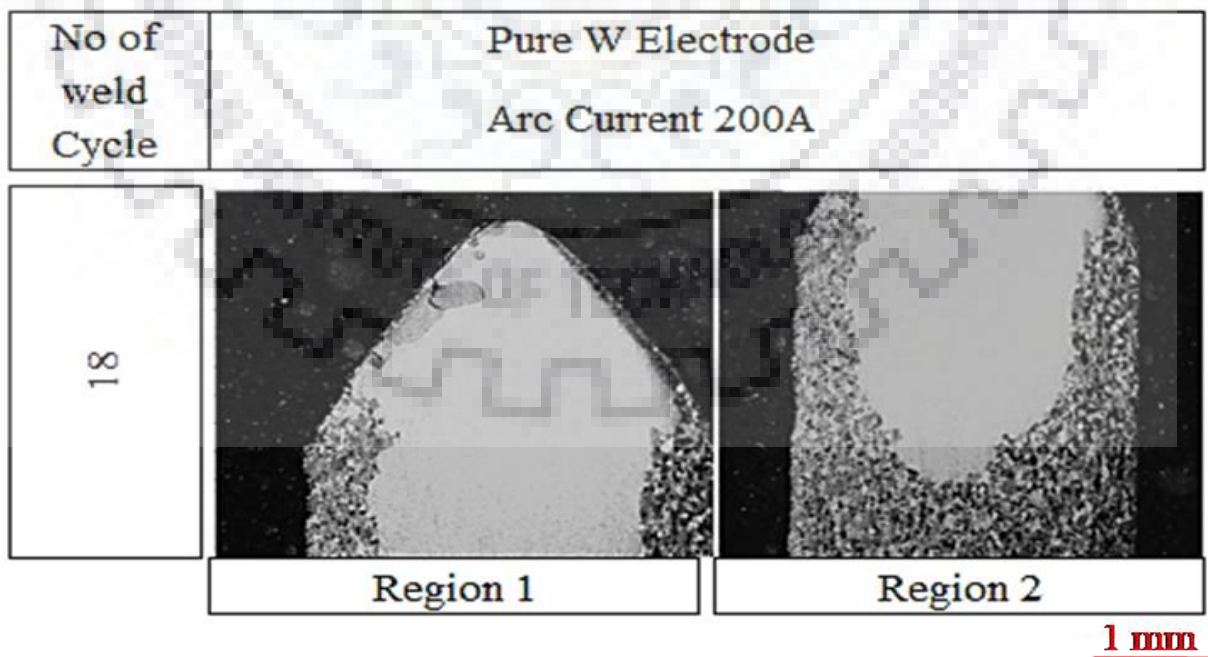


Figure 5.18: Metallurgical microstructures of an electrode cross section after 18 weld cycles

The metallurgical microstructures of pure tungsten electrode cross section are shown in Fig. 5.16, 5.17 and 5.18. The shown samples indicate the changes of inner structure with increasing weld cycles at 200 Ampere. It is clearly observed that:

1. Initially in the unused reference electrode, grains were longitudinal in the direction of electrode axis. As the arc was established, electrode started emitting electrons and the temperature of the electrode tip became very high due to resistive heating and arc plasma heating effect. Due to this very high temperature at the electrode tip in region A, as compared to the electrode bulk, grain coarsening took place in the prior one.
2. There is a drop in temperature from tip to clamping because of the lower effect of arc plasma heat and resistive heating in the cylindrical part. Moreover, radiation and convection heat losses are higher in the latter one.

When the arc was shut off, tungsten grains tended to recrystallize and formed granular equiaxed grains in region B. This is due to the fact that the former one had lesser temperature than the electrode tip that led to higher cooling rate of this region B. On the other hand, due to very slow cooling rate of electrode tip region A, single large grain was observed at the electrode tip.

3. As the number of weld cycles were increased up to 18 weld cycles, the single large grain which was observed at the electrode tip got bigger through the core of the electrode, while edges show granular grain structure.

It clearly indicates that before shut off of an arc, the temperature of the core of electrode was at higher than the surface.



5.3.2 SEM of electrode tip cross section

To study the effect of expansion and contraction due to arc switch off/on phenomena in interior/bulk of electrode tip, cross section of electrode tips were analyzed by SEM. Fig. 5.19 and 5.20 reveals that the inter granular cracks and voids are present not only on the surface but also present in the interior at higher weld cycles of 12 and 18

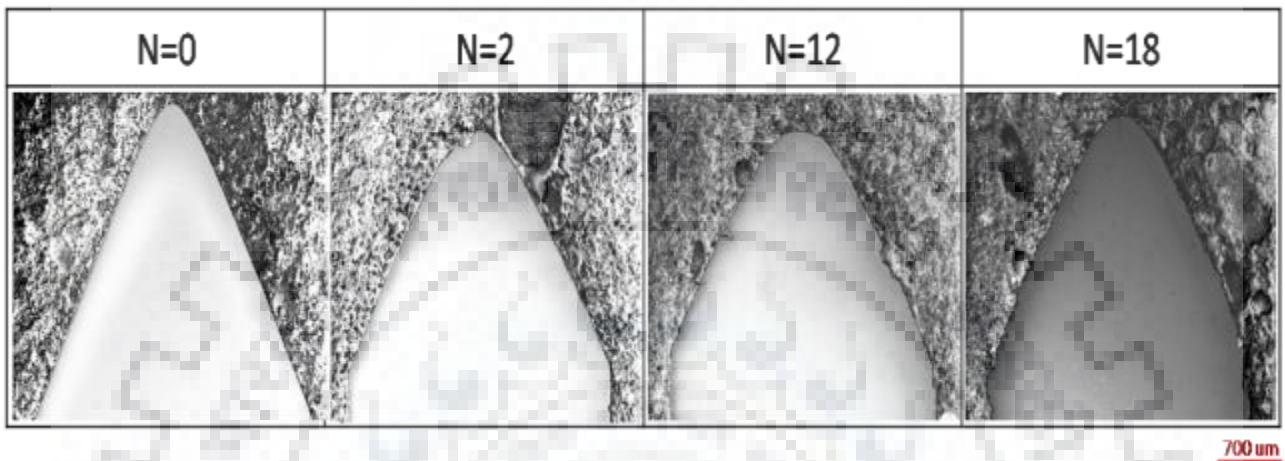


Figure 5.19: SEM micrographs of pure tungsten electrode tip after different weld cycles (N)

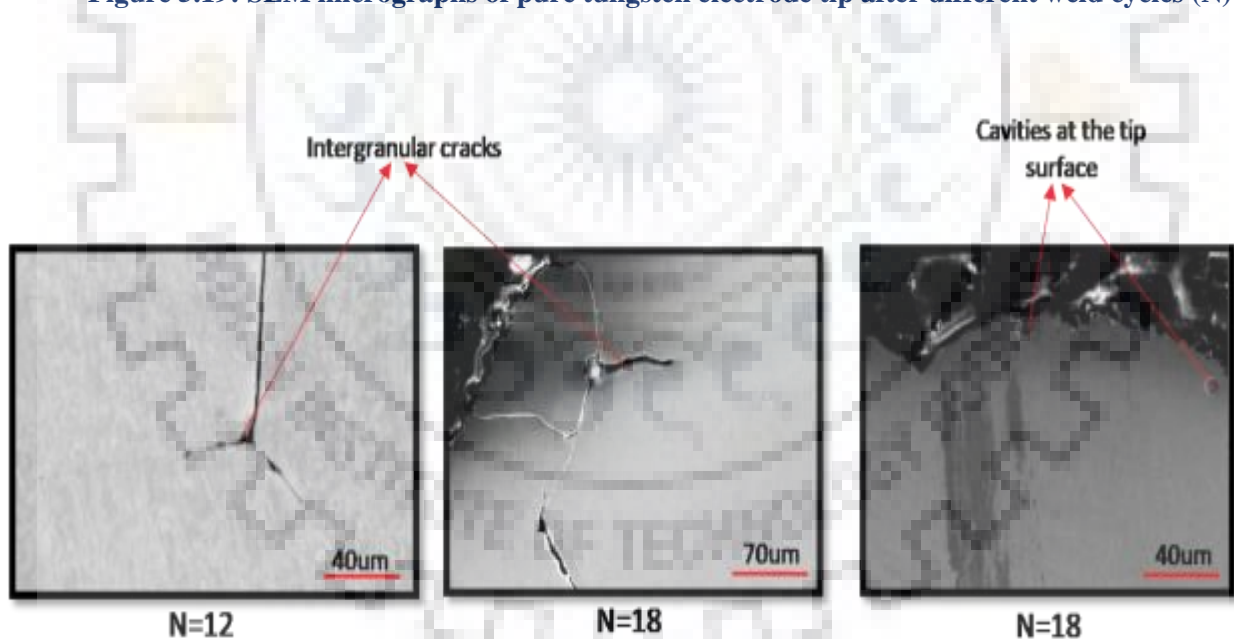


Figure 5.20: Magnified view of electrode tip cross section at higher weld cycles

5.4 Cross sectional study of Lanthanum oxide doped electrode tips

5.4.1 Optical microscopy of electrode tip cross section

Fig. 5.21 and 5.22 shows microstructure of Lanthanized electrode tip cross section after 30 and 60 minutes of arcing and it has been observed that:



1. Grain growth is higher at the tip and as well as the surface of zone C (as described in above topographical study) than the core of the electrode in contrary to pure tungsten electrode tips where core has higher grain growth.

This is because in lanthanized electrodes, presence of lanthanum oxide on the surface of the electrode reduces the melting point as well as recrystallization temperature of tungsten. Because of this decrease in recrystallization temperature, grain growth starts at lower temperature in comparison to pure tungsten electrode. The post flow of shielding gas after arcing is not able to control the surface grain growth in lanthanized electrode.

2. Lanthanised electrodes have still longitudinal grains present in the core because they are not re-crystallized unlike pure tungsten electrodes. In lanthanized electrodes La concentration is more at the surface as well as tip due to diffusion of lanthanum from centre to periphery of the electrode during arcing. Due to this diffusion, more concentration of Lanthana at the surface rather than the bulk which reduces recrystallization temperature of the surface. And these longitudinal grains with high number of grain boundaries are responsible for higher migration rate of La particles. Due to this migration rate, La particles are present at the tip providing a way to improve life of lanthanum doped electrodes.

3. Initially grain growth of surface of cylindrical part of the electrode and bulk is same. With increased weld cycles up to 12, grain growth is more at the surface of the upper part of electrode as shown in fig. It suggests that with increase in arcing time, upper part is also getting affected by the plasma and resistive heating.



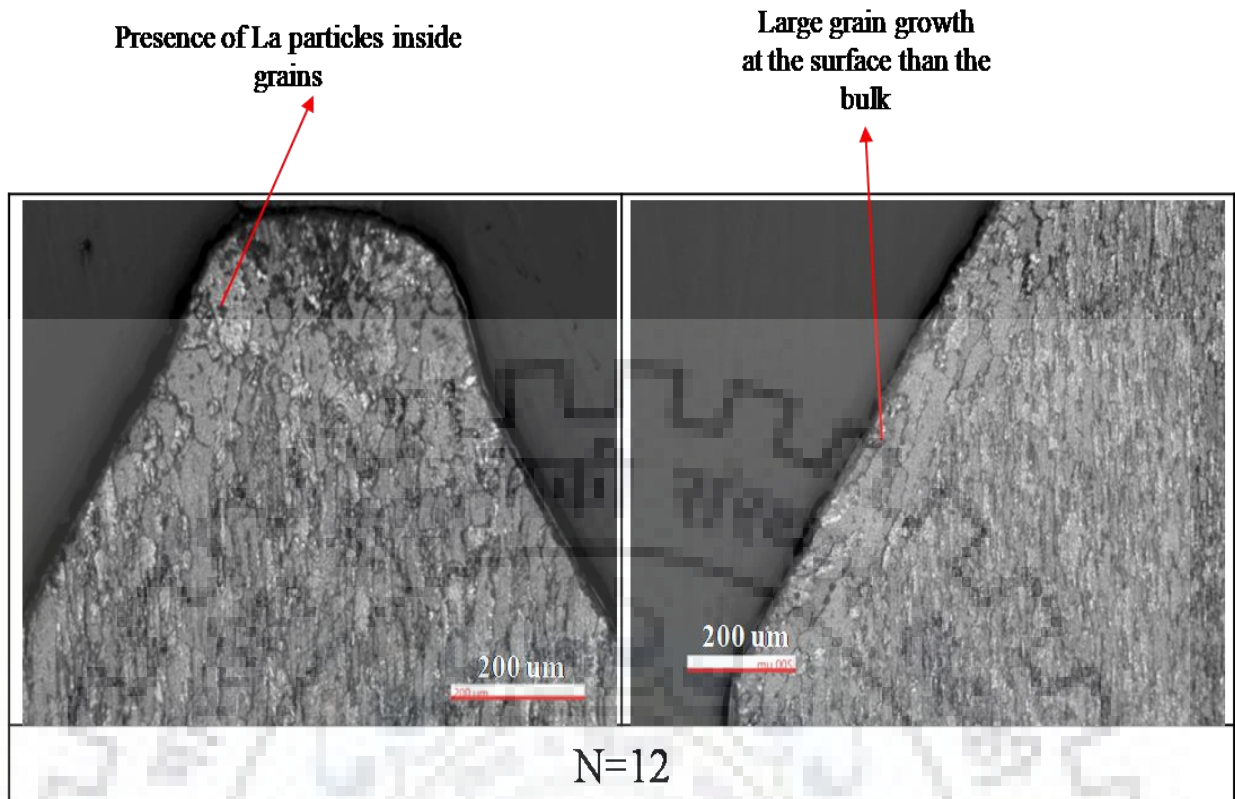


Figure 5.21: Optical microstructure of La doped electrode tips after 30 minutes of arcing (N=6)

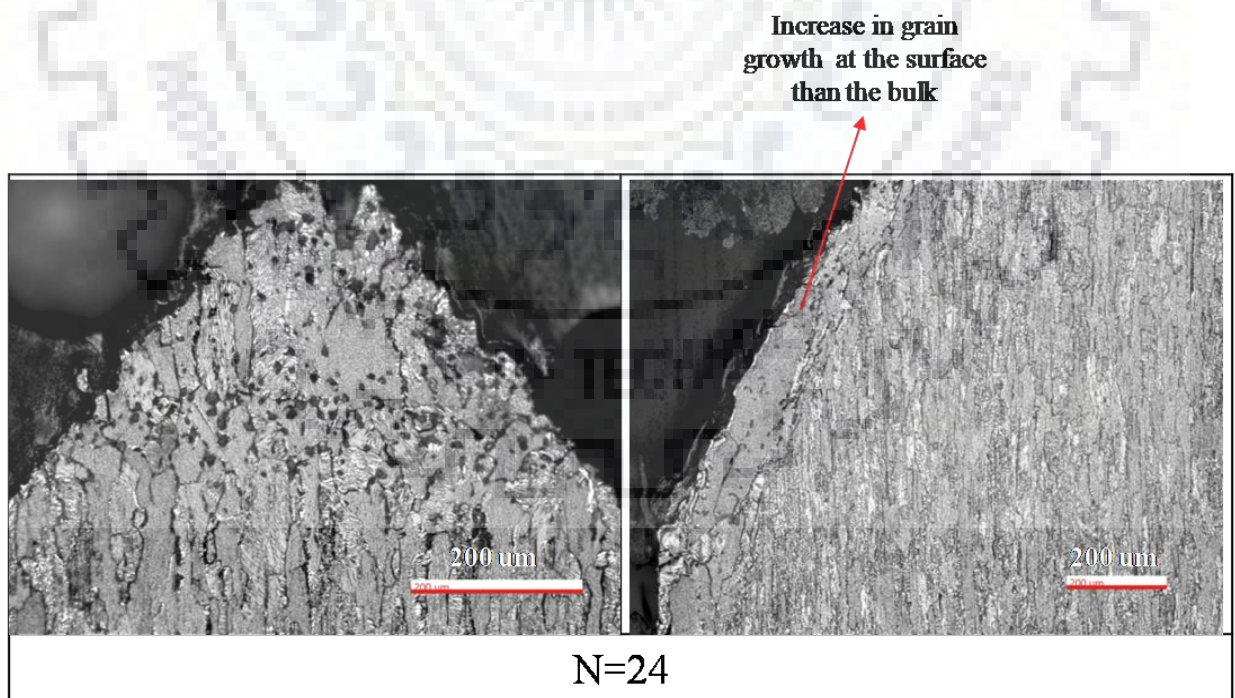


Figure 5.22: Optical microstructure of La doped electrode tips after 60 minutes of arcing (N=12)

5.4.2 SEM of Lanthanized electrode tip cross section

Fig. 5.23 shows cross-sectional microstructure of Lanthanized electrodes after 12 and 18 weld cycles. It has been observed that at the surface of zone C of electrode, shape of La particles are changing from the longitudinal to globular which also reveals the same that dissolution of La oxide particles is taking place and leads to formation of some phase.

And Fig 5.24 and Fig 5.25 shows EDX mapping of cross section of the tip and bulk of electrode tips after 12 and 18 weld cycles. It is observed that after 12 weld cycles, in the core of electrode, La particles shape is longitudinal as well as small globular. This globular shape of Lanthana clearly suggests that La is dissolving in tungsten and forming some phase. The formed phases is migrating to the tip from interior to electrode tip surface. With increased weld cycles up to 18, presence of Lanthana particles at the tip as well as globular La particles in the bulk are increasing. Increased in globular shape Lanthana reveals that more dissolution of La particles is taking place i.e., more formation of some new phase, that is leading to increased in migration rate of Lanthana to the electrode tip

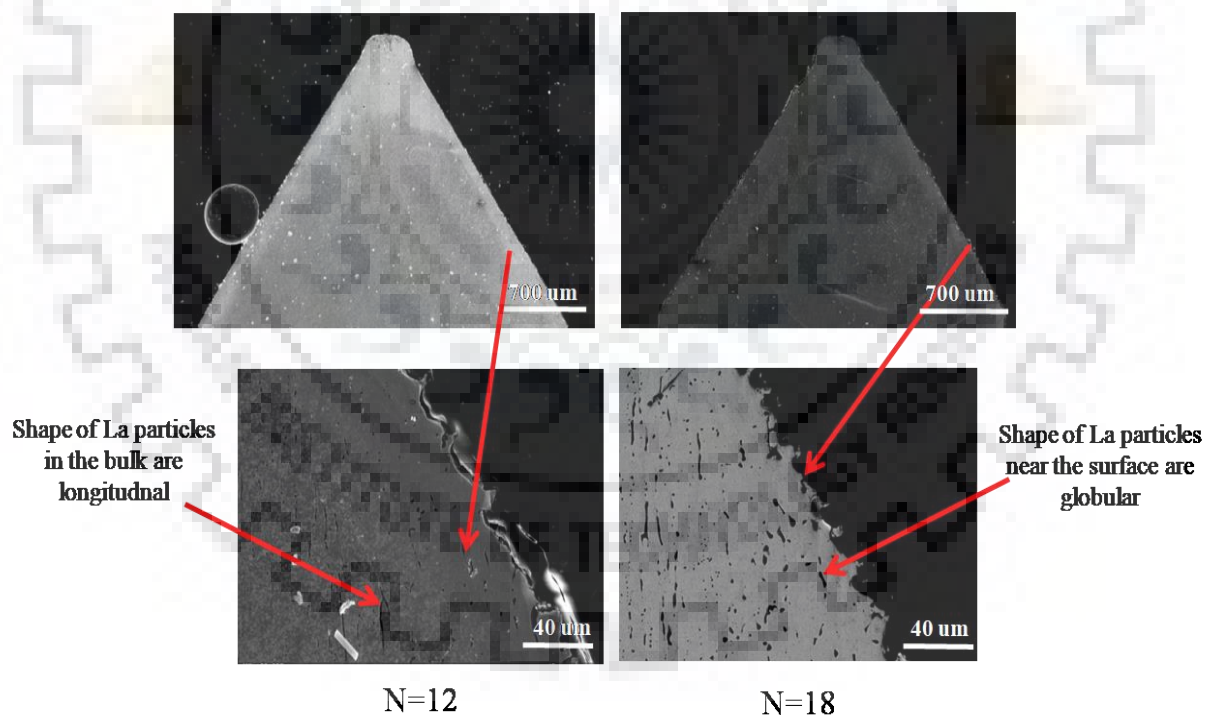


Figure 5.23: Microstructure of Lanthanised tip cross section after 12 and 18 weld cycles

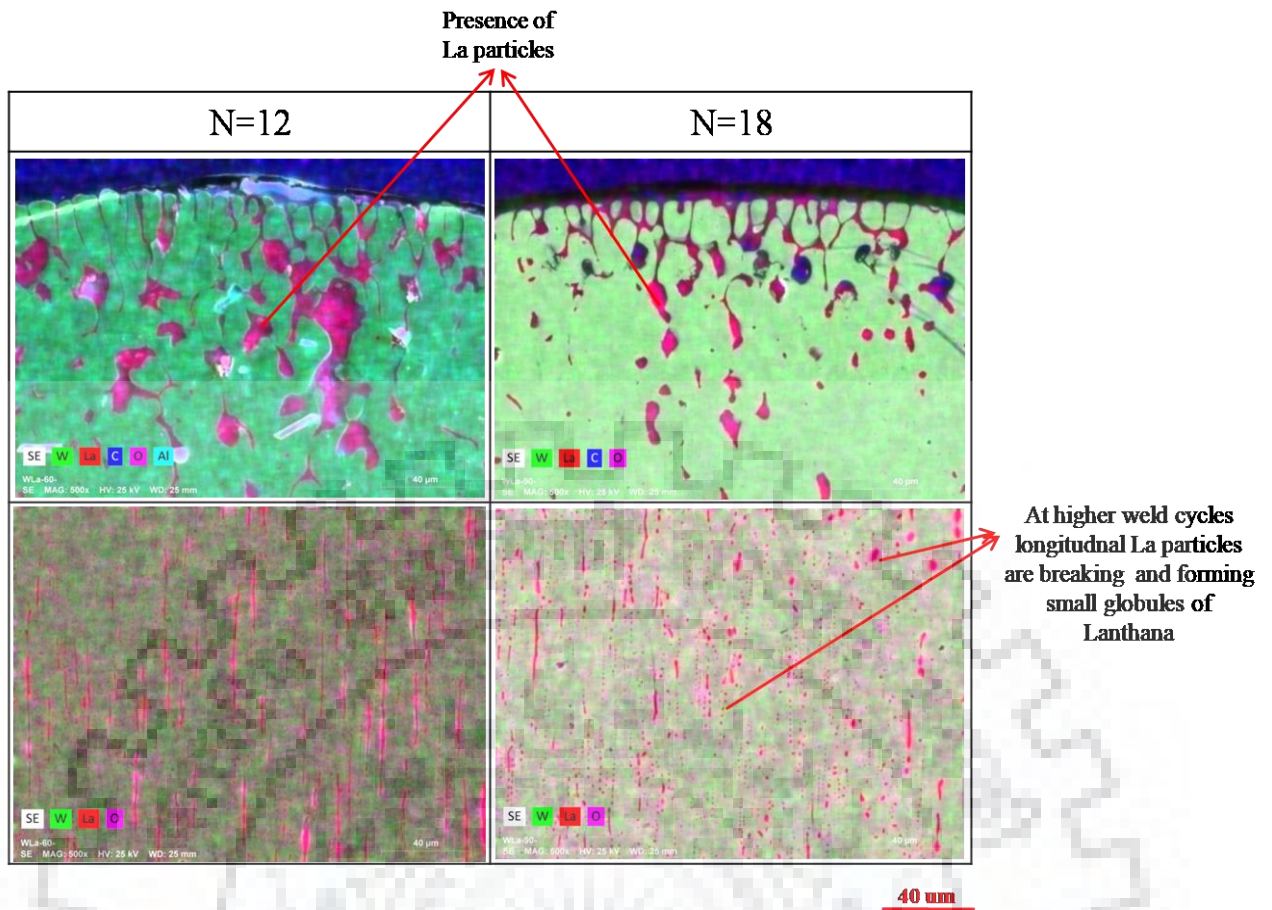


Figure 5.24: EDX mapping of electrode tip and core of electrode cross section after 12 and 18 weld cycles

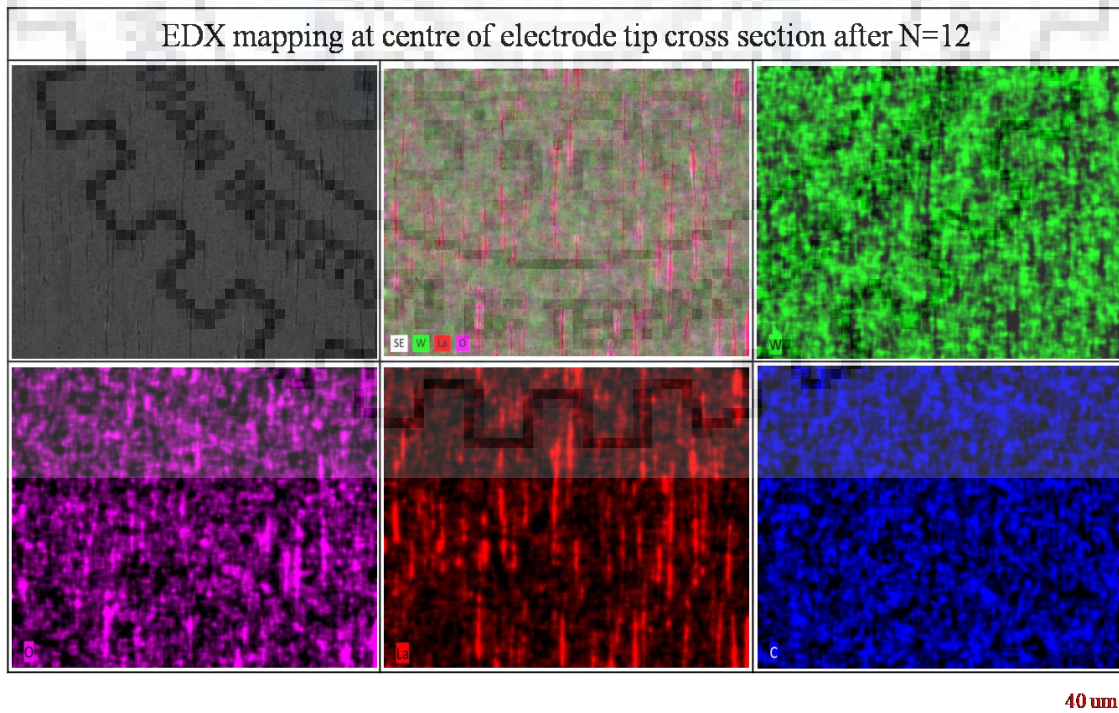


Figure 5.25: Elemental mapping at the center of electrode cross section after N=12

5.5 X-ray diffraction for phase analysis

EDX analysis of electrodes showed the presence of Lanthana on the tip as well as in the upper cylindrical part in the form of ring. It is important to know whether this La deposit is Lanthanum oxide or oxytungstates/tungstates reported in the literature. Electrodes were investigated by X-ray diffraction analysis for investigating the phases formed. Fig. 5.27 shows the XRD pattern for La_2O_3 doped electrodes at different weld cycles at 200 Ampere. It has been observed that:

1. The peak position and relative intensities in all XRD patterns matched with pure tungsten only. It is reported that during arcing La_2O_3 reacts with W, forming tungstates/oxytungstate. However, in the present case, no peaks of tungstates/oxytungstates or any other phases were found.
2. There are different possibilities that can explain the absence of Lanthanum-tungstate phases as describes in the literature.
 - One is that there are no such compounds were formed.
 - Second, phases could not be detected though present because of methodology in measurement. because there was no methodology described for XRD measurement by Osaka researchers. Also, XRD data reported [Source] is on the basis of 100 counts in which peak to background noise ratio was very large. There is a possibility that certain indications were misinterpreted as detections. A possible formation of the compounds cannot be surely concluded by considering of only these XRD data.

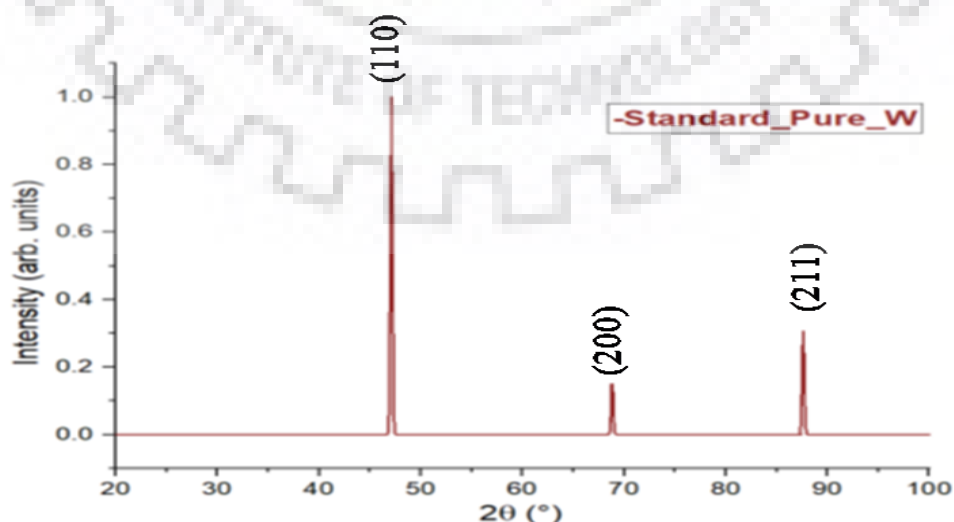


Figure 5.26: Standard XRD data of pure tungsten from IBSD database



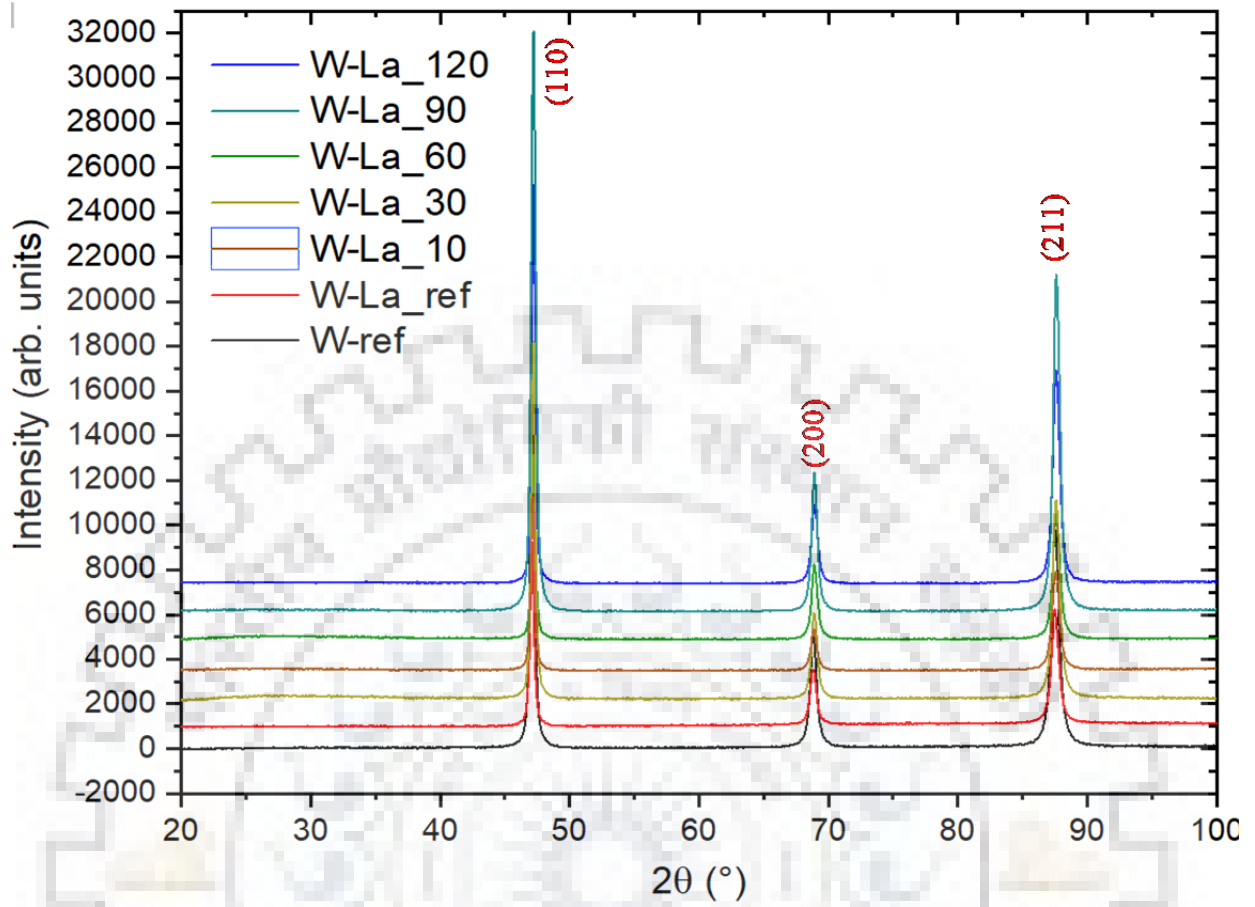


Figure 5.27: XRD analysis for Lanthanized electrodes after different weld cycles



6. CONCLUSION

From Optical Microscopy, Scanning electron Microscopy, Energy Dispersive Analysis and X-Ray Diffraction Analysis data obtained, following points can be concluded:

1. Erosion in pure tungsten electrode is higher than the lanthana doped tungsten electrode. In pure tungsten, erosion of electrodes is taking place by severe melting as well as evaporation process. The presence of larger grains due to high grain growth observed at electrode tip makes pure tungsten electrode less efficient.
2. While in the lanthana doped electrodes, erosion is taking place by high evaporation rate but with comparatively less melting. But it is still not well understood that whether tungstates are evaporating or Lanthanum oxide itself is evaporating. More data related to phase formation is needed.
3. Three characteristic zones have been observed in SEM of lanthana doped electrodes:
 - Zone A: Emission zone where migration rate of emitter particles is higher than their evaporation rate
 - Zone B: Lanthana depleted zone where evaporation rate is higher than migration rate.
 - Zone C: Crystallization zone where migration rate is higher than evaporation rate.
4. In cross sectional study of lanathana doped electrodes, the presence of globular shaped particles of lanthana reveals the dissolution of lanthana in tungsten matrix is taking place. This dissolution supports formation of some type of phases within the grains.
5. And optical microscopy of lanthanized electrodes shows the grain growth at surface of zone C and presence of lanthana inside the grains that is contrary to pure tungsten electrode in which grain growth is higher in the core of the electrode than its surface. This is because of the diffusion of lanthana from the center of the electrode towards the surface in Zone C in lanthanized electrode.
6. This contradiction in grain growth in both the electrodes and the evaporation of lanthana particles can be explained better by considering the data related to temperature distribution on the electrode surface and formation of phases between tungsten and lanthanum.



7. REFERENCES

1. Nie, Z., Chen, Y., Zhou, M. and Zuo, T., 2001. Research and Development of Tungsten Electrodes Added with Rare Earth Oxides.
2. Ushio, M., Sadek, A.A. and Matsuda, F., 1991. Comparison of temperature and work function measurements obtained with different GTA electrodes. *Plasma chemistry and plasma processing*, 11(1), pp.81-101.
3. Jeyaprakash, N., Haile, A. and Arunprasath, M., 2015. The parameters and equipments used in TIG welding: A review. *The international journal of engineering and science (IJES)*, 4(2), pp.11-20
4. Singh, P.K. and Kumar, P., 2015. A review on TIG welding for optimizing process parameters on dissimilar joints. *International Journal of Engineering Research and Applications*, 5(2), pp.125-128.
5. Little, R.L., 1973. Welding and welding technology.
6. Patel, A.B. and Patel, S.P., The Effect of Activating Flux in Tig Welding. *Editorial Committees*, p.65.
7. Patel, N.S. and Rahul, P.B., 2014. A review on parametric optimization of tig welding. *International Journal of Computational Engineering Research*, 4(1), pp.27-31.
8. Sathish, R., Naveen, B., Nijanthan, P., Geethan, K.A.V. and Rao, V.S., 2012. Weldability and process parameter optimization of dissimilar pipe joints using GTAW. *International Journal of Engineering research and applications*, 2(3), pp.2525-2530.
9. S V Nadkarni, Modern Arc Welding Technology, Ador Welding Limited, 2010, New Delhi.
10. Muncaster, P.W., 1991. *A practical guide to TIG (GTA) welding*. Elsevier.
11. Sadek, A.A., Ushio, M. and Matsuda, F., 1990. Effect of rare earth metal oxide additions to tungsten electrodes. *Metallurgical transactions A*, 21(12), pp.3221-3236.
12. Tseng, K.H. and Hsu, C.Y., 2011. Performance of activated TIG process in austenitic stainless steel welds. *Journal of Materials Processing Technology*, 211(3), pp.503-512.
13. Fletcher, M., 2009. Optimizing Tungsten Electrode Performance.



14. Tanaka, M., Tashiro, S., Nishikawa, H. and Ushio, M., 2007. Effective electrode work functions in argon gas tungsten arc during operation. *Surface and Coatings Technology*, 201(9-11), pp.5383-5386.
15. Florent Simonot: Abrasion of Tungsten electrode in real welding conditions, Thesis, Institute of Manufacturing and Assembly, TU Dresden
16. McCarthy, P.T., Reifenberger, R.G. and Fisher, T.S., 2014. Thermionic and photo-excited electron emission for energy-conversion processes. *Frontiers in Energy Research*, 2, p.54.
17. Sadek, A.A., Ushio, M. and Matsuda, F., 1990. Effect of rare earth metal oxide additions to tungsten electrodes. *Metallurgical transactions A*, 21(12), pp.3221-3236.
18. Ushio, M., Sadek, A.A. and Matsuda, F., 1991. Comparison of temperature and work function measurements obtained with different GTA electrodes. *Plasma chemistry and plasma processing*, 11(1), pp.81-101.
19. Ogawa, K., Suga, Y. and Matsumoto, H., 1992. Erosion characteristics of tungsten electrodes in TIG arc welding.
20. Matsuda, F. and Ushio, M., 1990. Effects of combined additives of rare earth metal oxides on arc characteristics of tungsten electrodes. *Transactions of the Japan welding Society*, 21(2).
21. Casado, E., Colomer, V., Muñoz-Serrano, E. and Sicilia, R., 2002. An experimental comparison of the erosion in tungsten cathodes doped with different rare-earth elements. *Journal of Physics D: Applied Physics*, 35(10), p.992.
22. Li, P., Yang, J. and Li, Y., 2017, May. Welding Performance of Several New Rare Earth Tungsten Electrodes. In *Materials Science Forum* (Vol. 898).

